# Ocean Barramundi Expansion Project - Model Calibration Report

| | |
|---|---|
| Customer | Tassal |
| Project | 175801.000 |
| Deliverable | 4 |
| Version | 1 |
| | 20 June 2024 |

# Document Control

## Document Identification

| | |
|---|---|
| Title | Ocean Barramundi Expansion Project - Model Calibration Report |
| Project No | 175801.000 |
| Deliverable No | 4 |
| Version No | 1 |
| Version Date | 20 June 2024 |
| Customer | Tassal |

| | |
|---|---|
| Author | Alexander Waterhouse, Kabir Suara and Gayan Gunaratne |
| Reviewed By | Louise Bruce |
| Project Manager | Harrison Carmody |

## Amendment Record

The Amendment Record below records the history and issue status of this document.

| Version | Version Date | Distribution | Record |
|---|---|---|---|
| A | 27 March 2022 | Internal | Review |
| 0 | 03 May 2022 | Client | BMT report |
| 1 | 20 June 2024 | Client | BMT report |

# Contents



## Tables



## Figures

# 1 Overview

An integrated 3-D hydrodynamic water quality and sediment diagenesis model of the Kimberley coastal and offshore region was developed to support the Environmental Impact Assessment (EIA) Tassal's proposed farming expansion plans to the proposed sites in the Buccaneer Archipelago. This report describes the methods used in the integrated model calibration and verification process and details the results of model comparisons against observed data. Further information pertaining to the integrated model have been included in the following reports:

- Ocean Barramundi Project – Baseline Marine Environmental Quality Study (BMT 2024a): Details the methods and data collected during baseline hydrodynamic water and sediment quality monitoring program. These data were used in the calibration process to compare against the model outputs for baseline (pre-farming) scenario.

- Ocean Barramundi Project – Integrated Modelling Report (BMT 2024b): Describes the dynamics of the integrated aquaculture models used to examine the impact of the proposed farm operations as well as the results of the scenario model outputs used to support the EIA.

The region surrounding the proposed sites is a dynamic system influenced by largescale to local processes. Simulating such an environment is challenging, as a model must resolve the dynamic processes affecting the area on a regional scale (e.g., regional currents), the mesoscale (e.g., eddy formation) and the local scale (e.g., the influence of local bathymetric features on current velocities). The EIA process entails the calibration of hydrodynamic and water quality models of the area to quantify the potential impacts of aquaculture activities on water quality parameters (e.g., nutrient concentrations, chlorophyll-a concentrations, etc.) against pre-farming baseline conditions. The model calibration and verification simulations covered two periods from February-August 2021 to replicate the field monitoring programs conducted in representative wet and dry seasons. Further validation of the additional baseline monitoring program was conducted to verify conditions were similar between the two monitoring programs (BMT 2024a). For calibration, only one monitoring program period could be selected, noting the model itself only runs for a period of 12 months, and the two monitoring programs are non-continuous. As such, the first period was selected noting it occurred at the same time as the hydrodynamic baseline collection, as well as the fact that the model had already been calibrated previously.

The results of the hydrodynamic calibration demonstrated that the hydrodynamic model was successful in replicating the physical processes observed in the Buccaneer Archipelago and was deemed "fit for purpose" in simulating the fate of particles released from aquaculture activities and providing a realistic hydrodynamic regime to force the water quality module. Additionally, the water quality model recreated the predominantly oligotrophic conditions across the simulated period. As such, the water quality model was deemed 'fit-for-purpose' in assessing the effects of aquaculture activities against baseline for water quality impacts within the area of interest.

Section 2 and Section 3 of this Report presents the results of hydrodynamic and water quality model calibration respectively.

# 2 Hydrodynamic model calibration

## 2.1 Overview

The primary aims of the hydrodynamic model were to provide a representation of currents for determining the fate and transport of the waste released from the aquaculture activities and temperature gradients for simulating ecosystem processes including the sediment diagenesis model through its temperature dependence functions. The hydrodynamic model calibration process was therefore focussed on water levels, currents (including riverine flow discharge) and temperature. Model calibration was achieved by finetuning mesh resolution and adjusting bed flow resistance and bathymetry offsets to achieve a desired level of model performance.

A brief description of the field observations, the performance metrics used in comparing the model to the observations and the results of these comparisons are presented.

## 2.2 Field observations

### 2.2.1 Fixed ADCPs

Three Acoustic Doppler Current Profilers (ADCPs) were deployed between Strickland Bay to Yampi Sound to guide model calibration and validation. All three ADCPs were deployed over the same period from 10th of April through to 15th of May 2021. The location of the ADCP deployments used in the calibration process are listed in Table 2.1 and depicted in Figure 2.1. Note that the data collected from the Sontek was excluded from the calibration process as the model mesh was too course to resolve the complexity of currents in that location.

Table 2.1 ADCP Deployments

| ADCP Name | Location Coordinates | Sampling Characteristics |
|---|---|---|
| RDI1 | Lon: 123.67834°<br>Lat: -16.14446° | sampling interval:<br>n. bins:<br>bin size: 0.75m<br>height of first bin: |
| RDI2 | Lon: 123.57677°<br>Lat: -16.36761° | sampling interval:<br>n. bins:<br>bin size: 0.75m<br>height of first bin: |
| Sontek | Lon: 123.52471°<br>Lat: -16.18878° | sampling interval:<br>n. bins:<br>bin size: 0.75m<br>height of first bin: |

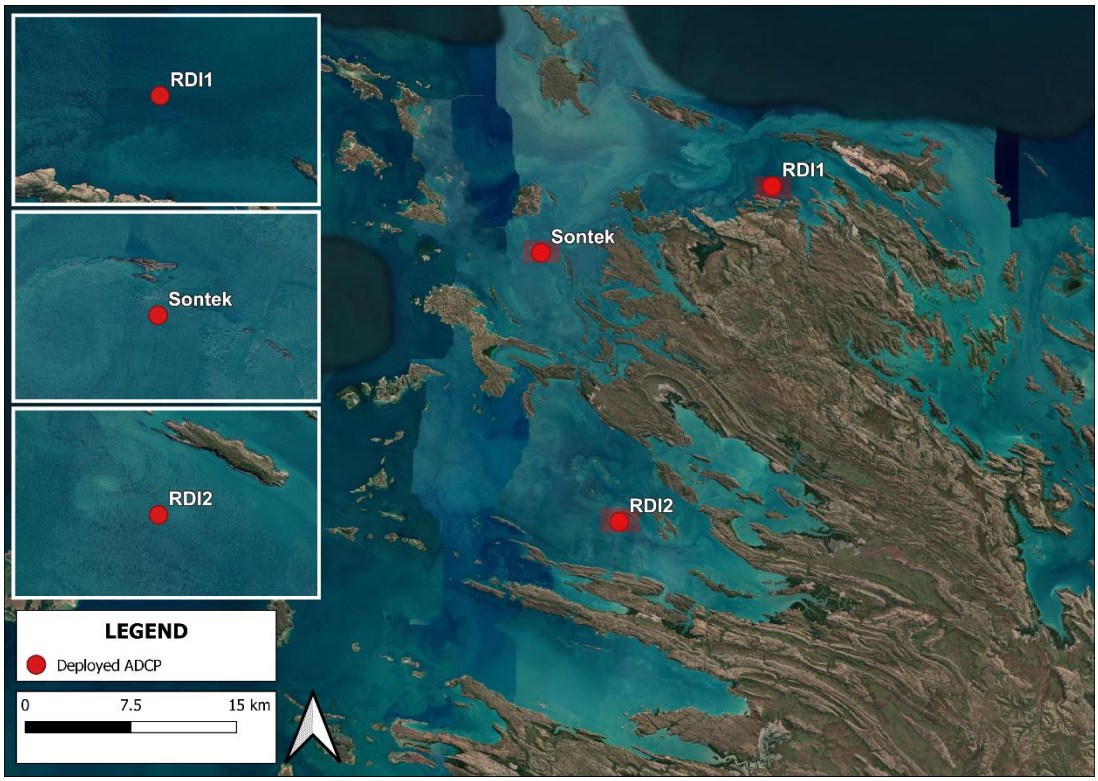


Figure 2.1 ADCP deployment locations and zoomed inserts.

### 2.2.2 ADCP Transects

ADCP transect measurements were undertaken using a boat mounted ADCP to measure current magnitude and speed across a tidal cycle. Three locations were chosen for the transect measurements (refer Figure 2.2):

- Koolan (northern transect), located between Koolan Island and the mainland,
- Bayliss (central transect), located between Bayliss Island and Hidden Island, and
- Strickland (southern transect), located in Strickland Bay between Aveling Island and Edeline Island.

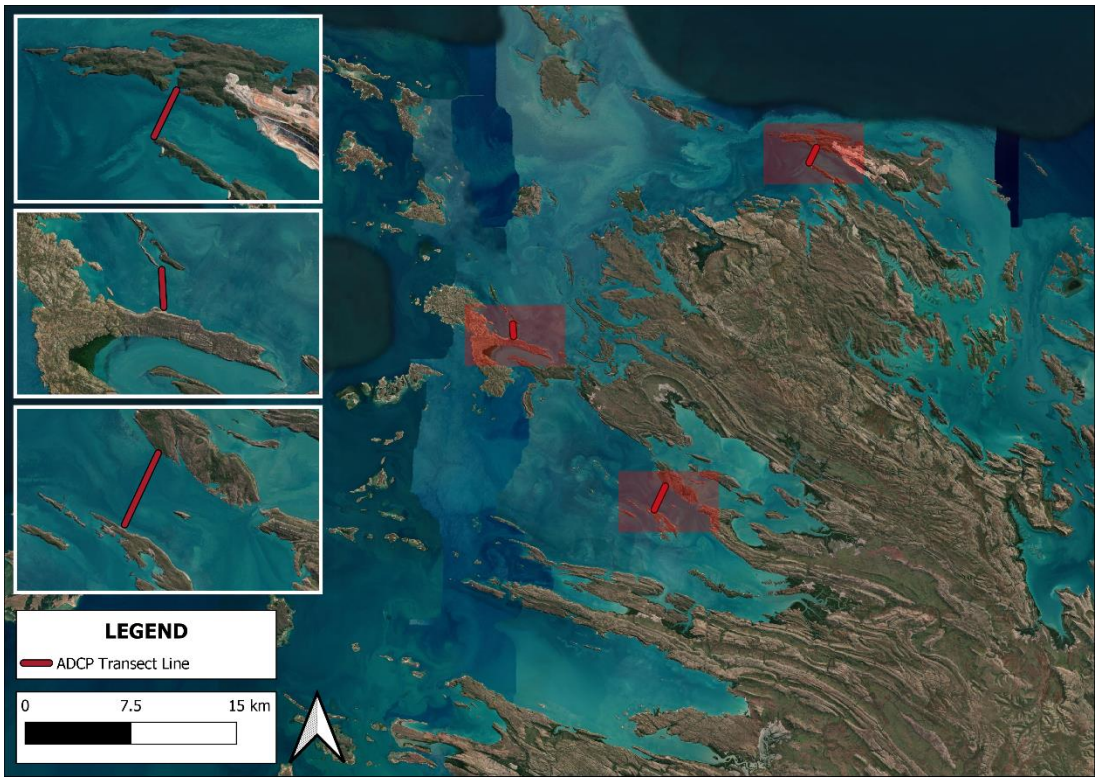


Figure 2.2 Locations of ADCP transects. Left panel inserts depict transects from top to bottom Koolan, ii) Bayliss, and iii) Strickland.

## 2.3 Model performance metrics

Three model performance metrics were used to guide model calibration, including:

- Index of Agreement (IOA),
- Mean Absolute Error (MAE), and
- Root Mean Square Error (RMSE).

The IOA was originally developed by Willmott (1981) and subsequently modified in Willmott et al. (1985):

$$IOA = 1 - \frac{\sum_{i=1}^{N} |O - P|^2}{\sum_{i=1}^{N} (|P - \bar{O}| + |O - \bar{O}|)^2}$$

where *O* is the observed data and *P* is the model predictions over a given time period divided into *N* increments. The overbar denotes the time averaged mean of the given variable. Following Willmott (1981) and Willmott *et al.* (1985), the IOA can vary from 0 to 1 with higher values indicating better model predictive skill. While there are no generic guidelines for the interpretation of the IOA, a value above 0.5 is generally considered to indicate satisfactory model performance.

The MAE and RMSE were adopted to quantify the model error in dimensional units and provide a measure of model performance on an average sense, with RMSE showing bias to larger discrepancies. The MAE and RMSE are computed as follows:

$$MAE = N^{-1} \sum_{i=1}^{N} |O - P|$$

$$RMSE = \left( N^{-1} \sum_{i=1}^{N} (O - P)^2 \right)^{1/2}$$

In addition to statistical analysis of model performance visual comparisons between modelled and measured water levels, velocities, and temperature were undertaken for the months of April and May 2021.

## 2.4 Water levels

Water level comparisons were made against both AusTides tidal data and water levels extracted from the ADCP deployments.

### 2.4.1 AusTides comparisons.

Comparison of modelled water levels were made against AusTides water level predictions (Australian Hydrographic Office) data at the following five stations in the Buccaneer Archipelago:

- Yampi Sound
- Bedford Islands
- Macleay Island
- Sunday Island
- Derby.

These predictions are considered highly accurate and provide a good source of long-term water-level data for calibration purposes.

Figure 2.3 through Figure 2.7 show the comparison between the water level predicted by the hydrodynamic model and AusTides predictions at various stations. The quantitative metrics for these plots are provided in Table 2.2.

The model closely reproduced the tidal phases at all locations across the spring tidal cycle. The model tended to underpredict the water level peaks and troughs at Macleay, Sunday and Derby Islands with

largest deviation of ~0.5 m recorded in Derby Island where the tidal range was greater than 10 m. Comparisons show a very good agreement between the modelled and predicted water levels at Yampi Sound and Bedford Islands. Overall, the model compared well with AusTides water level as reflected in the error metrics with RMSE errors generally less than 0.5 m and an IOA of at least 0.99.

Table 2.2 AusTides predicted water-level validation scores

| Station | IOA | RMSE (m) | MAE (m) |
|---|---|---|---|
| Yampi Sound | 1.0 | 0.21 | 0.17 |
| Bedford Islands | 0.99 | 0.38 | 0.31 |
| Macleay Island | 0.99 | 0.45 | 0.37 |
| Sunday Island | 0.99 | 0.39 | 0.33 |
| Derby | 0.99 | 0.51 | 0.43 |

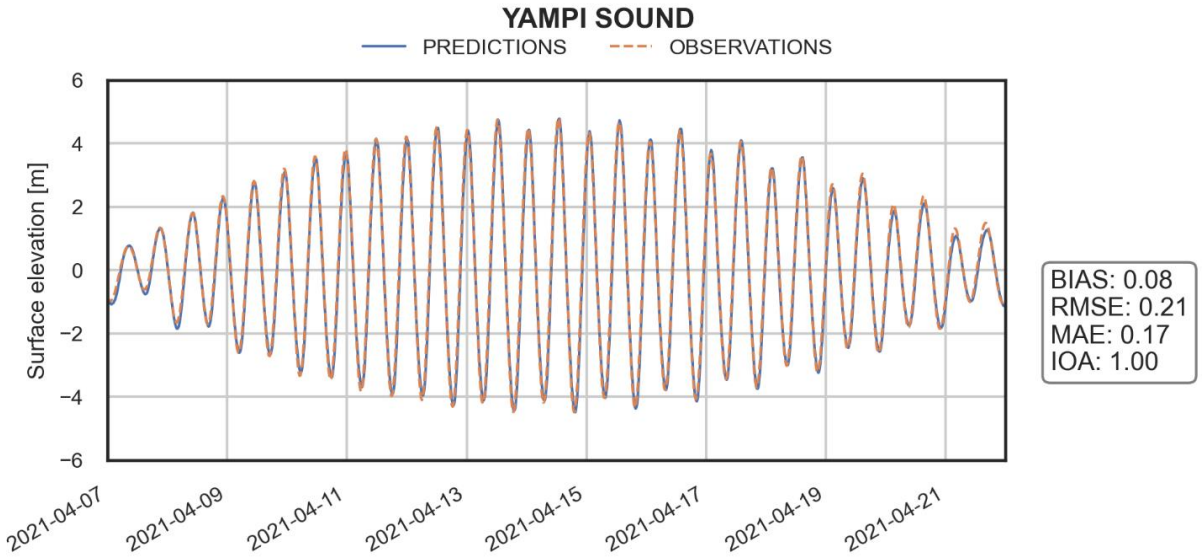


Figure 2.3 Water-level comparison at Yampi Sound showing predicted and modelled water-levels

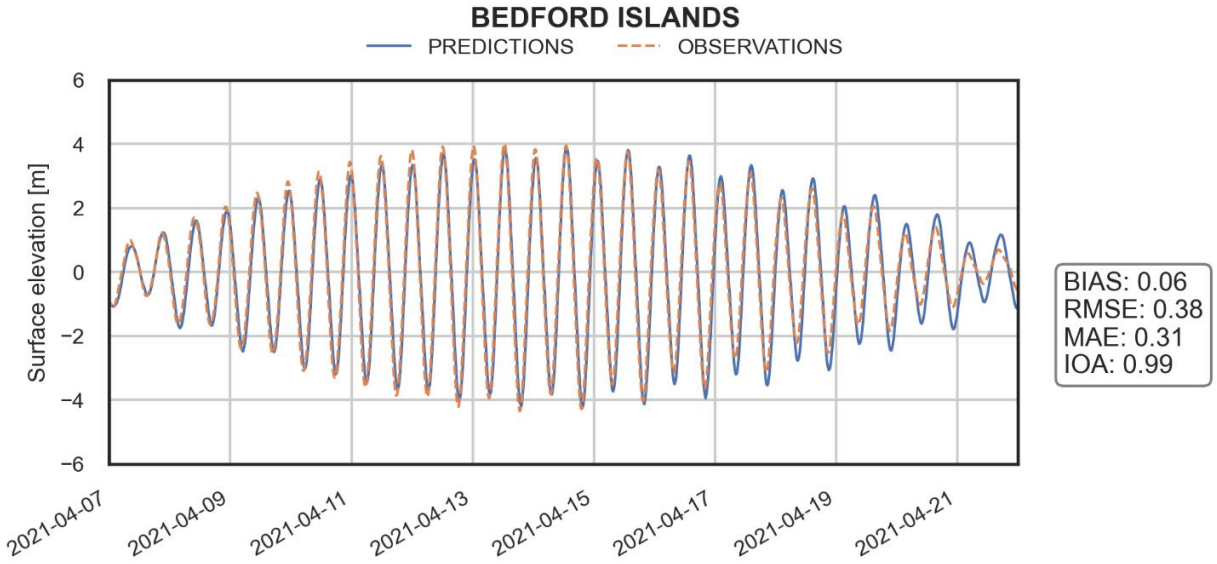


Figure 2.4 Water-level comparison at Bedford Islands showing predicted and modelled water-levels

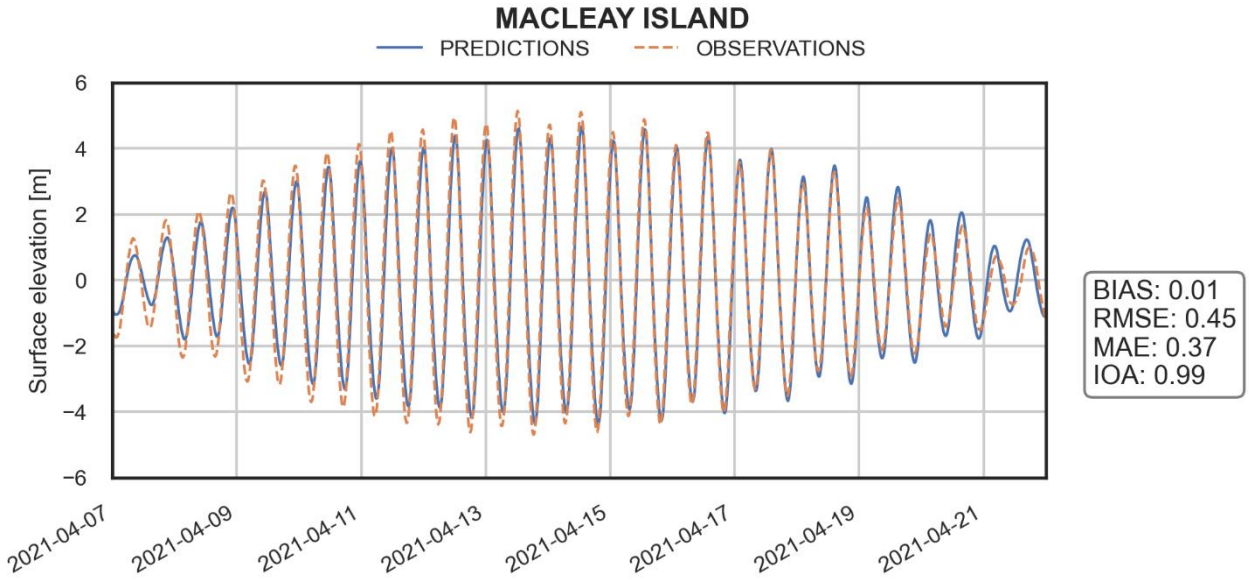


Figure 2.5 Water-level comparison at Macleay Island showing predicted and modelled water-levels

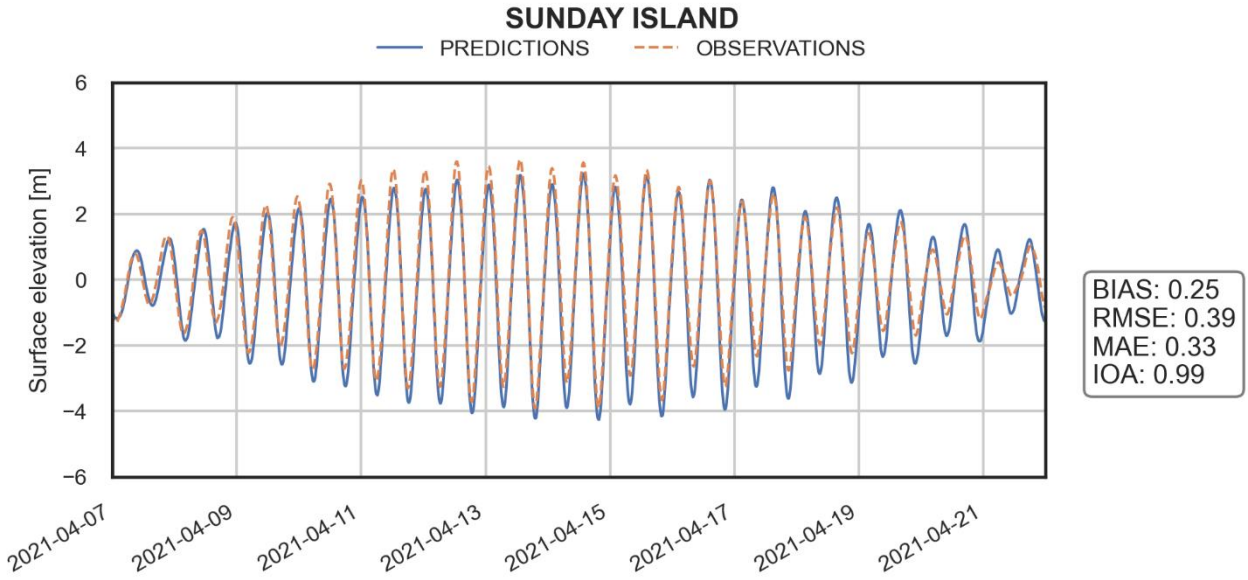


Figure 2.6 Water-level comparison at Sunday Island showing predicted and modelled water-levels

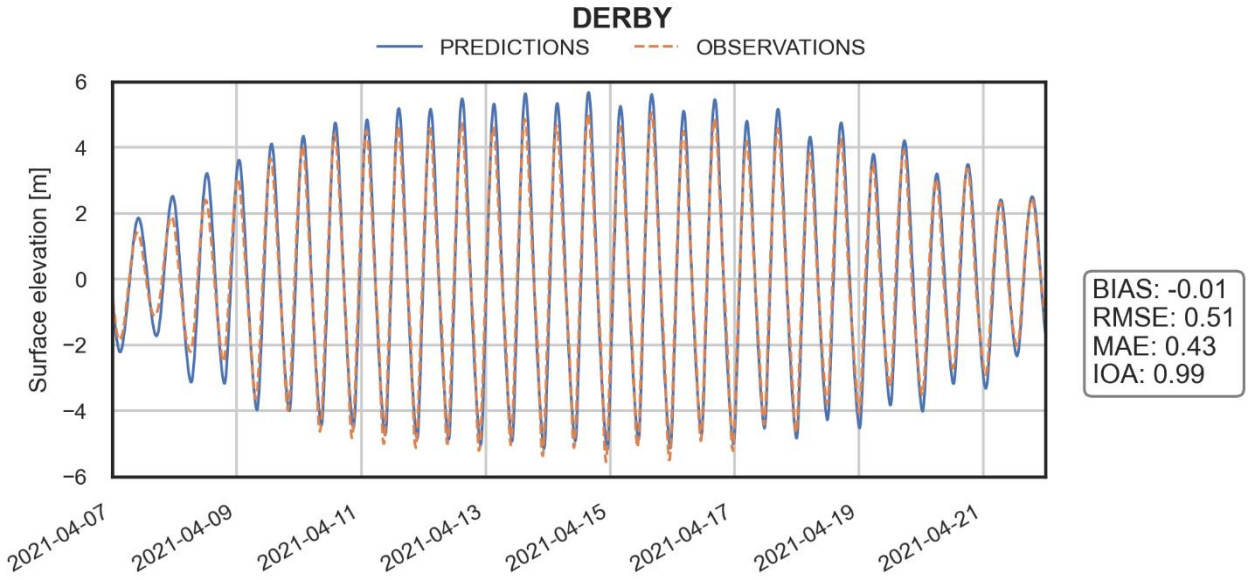


Figure 2.7 Water-level comparison at Derby showing predicted and modelled water-levels

### 2.4.2 ADCP Water-level measurements

Two ADCPs, RDI1 and RDI2 measured water-level during the deployment and provided additional verification for accuracy of modelled water level predictions.

Water level comparisons between the model and ADCP measurements are shown in Figure 2.8 and Figure 2.9 and model performance statistics are listed in Table 2.3. The model overpredicted the peaks and troughs of water level for RDI1 by ~0.5 m and underpredicted at RDI2 by ~0.3m. Note that given the large tidal range (>10 m) for the regions, these discrepancies are relatively small. In general, the

model demonstrated a strong agreement with the ADCP field measurements with RMSE errors of 0.4 m and IOA's of 0.99.

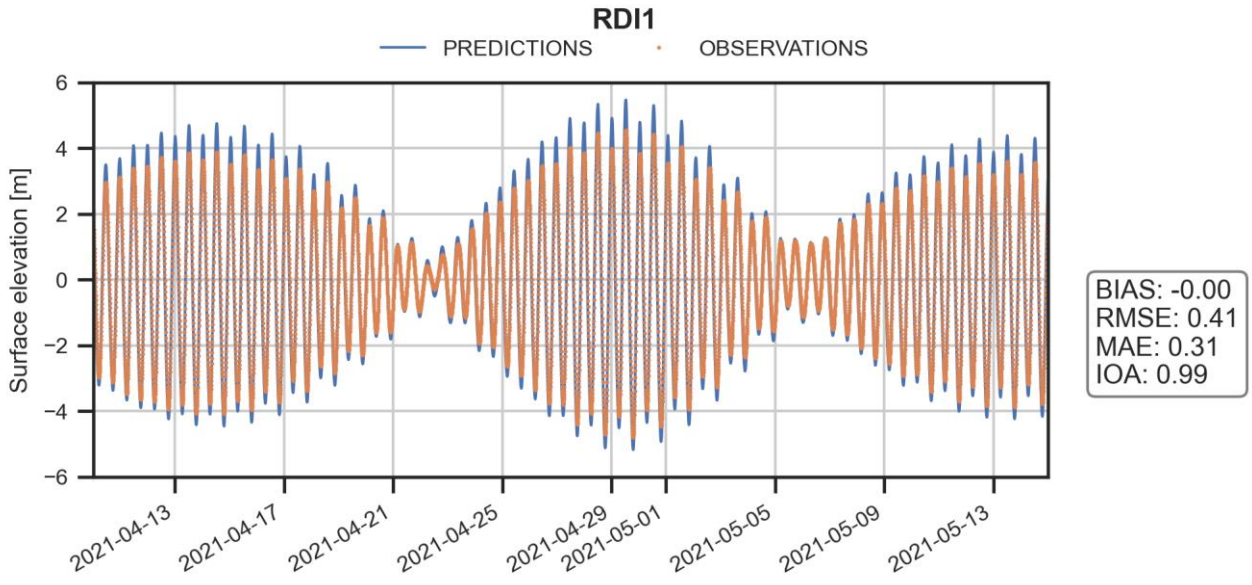


Figure 2.8 Water-level comparison at RDI1 showing measured and modelled water-levels

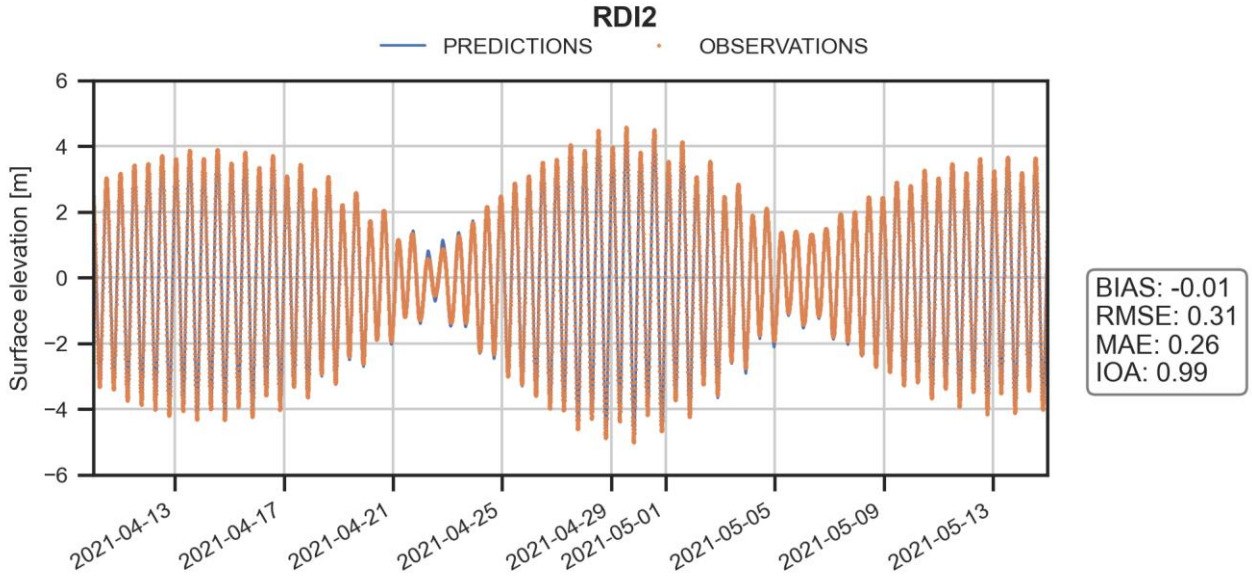


Figure 2.9 Water-level comparison at RDI2 showing measured and modelled water-levels

Table 2.3 ADCP Water-level model performance scores

| Station | IOA | RMSE (m) | MAE (m) |
|---|---|---|---|
| RDI1 | 0.99 | 0.41 | 0.31 |
| RDI2 | 0.99 | 0.31 | 0.26 |

## 2.5 Velocity

Visual and quantitative comparisons of modelled and measured velocity were undertaken for the period of April and May 2021 using the following data sources and methods:

- Fixed point depth-averaged current comparisons against the fixed ADCPs (RDI1 and RDI2),
- Fixed point current profile comparisons against the fixed ADCPs (RDI1 and RDI2),
- ADCP transect comparisons measured at Bayliss Island, Koolan Island and Strickland Bay.

### 2.5.1 Depth-averaged currents

Depth averaged comparisons for RDI1 and RDI2 are shown in Figure 2.10 and Figure 2.11 respectively including modelled and measured current speed and direction, with performance statistics listed in Table 2.4.

Velocity magnitudes and directions were replicated moderately well by the model with good IOA > 0.9 for both magnitude and direction. The time variations in the velocity components across the locations were closely replicated by the model. Furthermore, the tidal velocities and spring-neap modulation were closely replicated in both locations. The visual inspection and performance metrics (Table 2.4) with RMSE < 0.06 m/s and MAE < 0.04 m/s from RDI1 and RDI2 show that the model closely replicated recorded velocities.

Table 2.4 Performance metrics for depth-averaged velocity

| Station | IOA | RMSE (m/s / °) | MAE (m/s / °) |
|---|---|---|---|
| **Current Speed (m/s)** | | | |
| RDI1 | 0.93 | 0.06 | 0.04 |
| RDI2 | 0.90 | 0.06 | 0.05 |
| **Current Direction (°)** | | | |
| RDI1 | 0.91 | 49.32 | 34.63 |
| RDI2 | 0.95 | 43.55 | 22.25 |

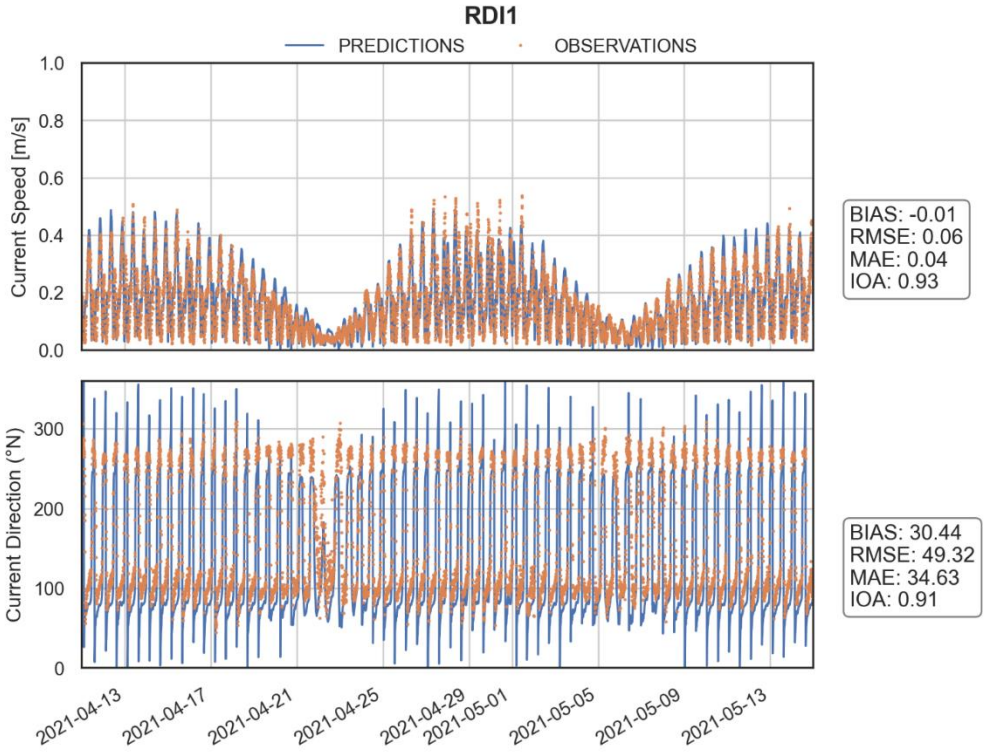


Figure 2.10 Velocity comparison at RDI1 showing measured and modelled current speed and current direction

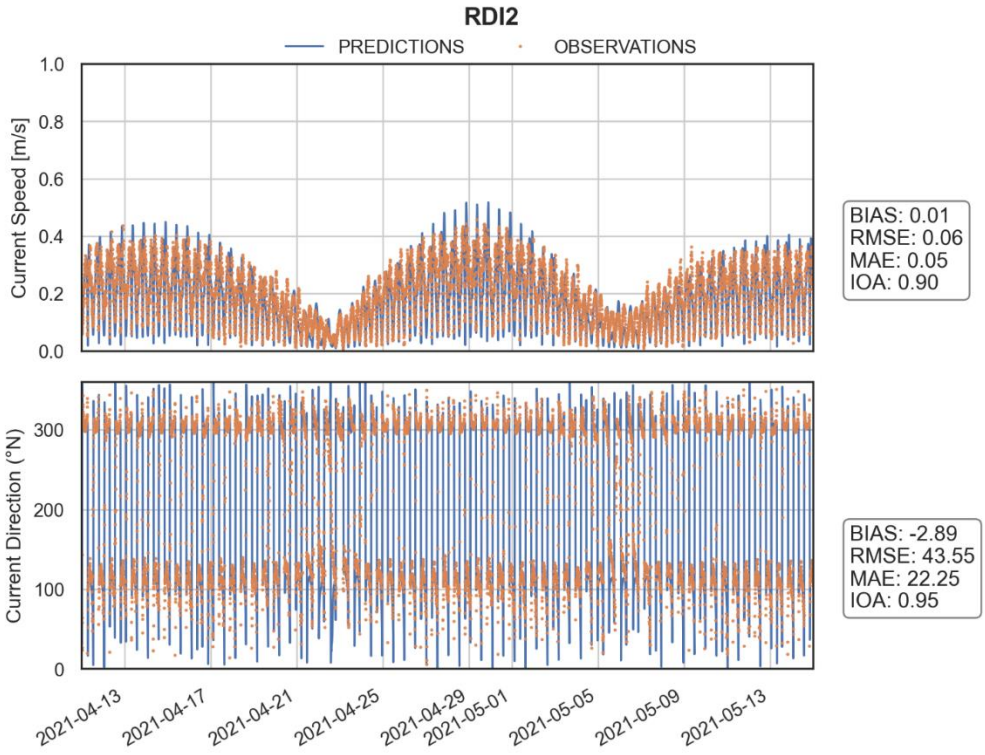


Figure 2.11 Velocity comparison at RDI2 showing measured and modelled current speed and current direction

### 2.5.2 Current Profiles

Current profiles at RDI1 and RDI2 locations are presented in Figure 2.12 through to Figure 2.15. These figures show current speed throughout the water-column along the east-west and north-south directions. The figures provide a qualitative comparison between the model prediction and observed components of the velocity. Consistent with quantitative metric presented above for the depth averaged velocity magnitude and direction, the depth profiles of velocity components were closely replicated by the model at the two locations.

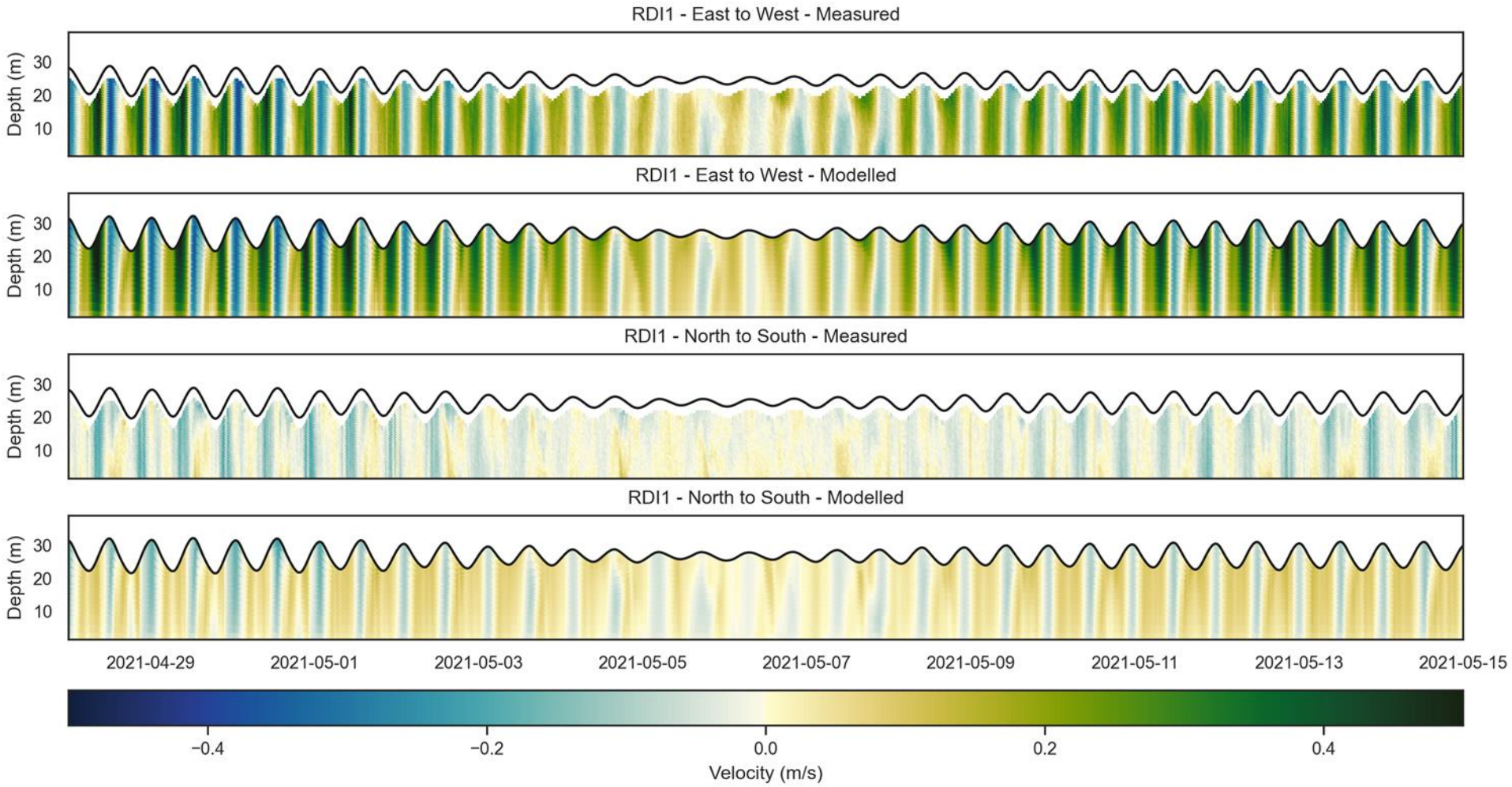


Figure 2.12 Current profiles at RD1 from April 28th to May 15th 2021 showing comparison between measured and modelled east-west and north-south velocity

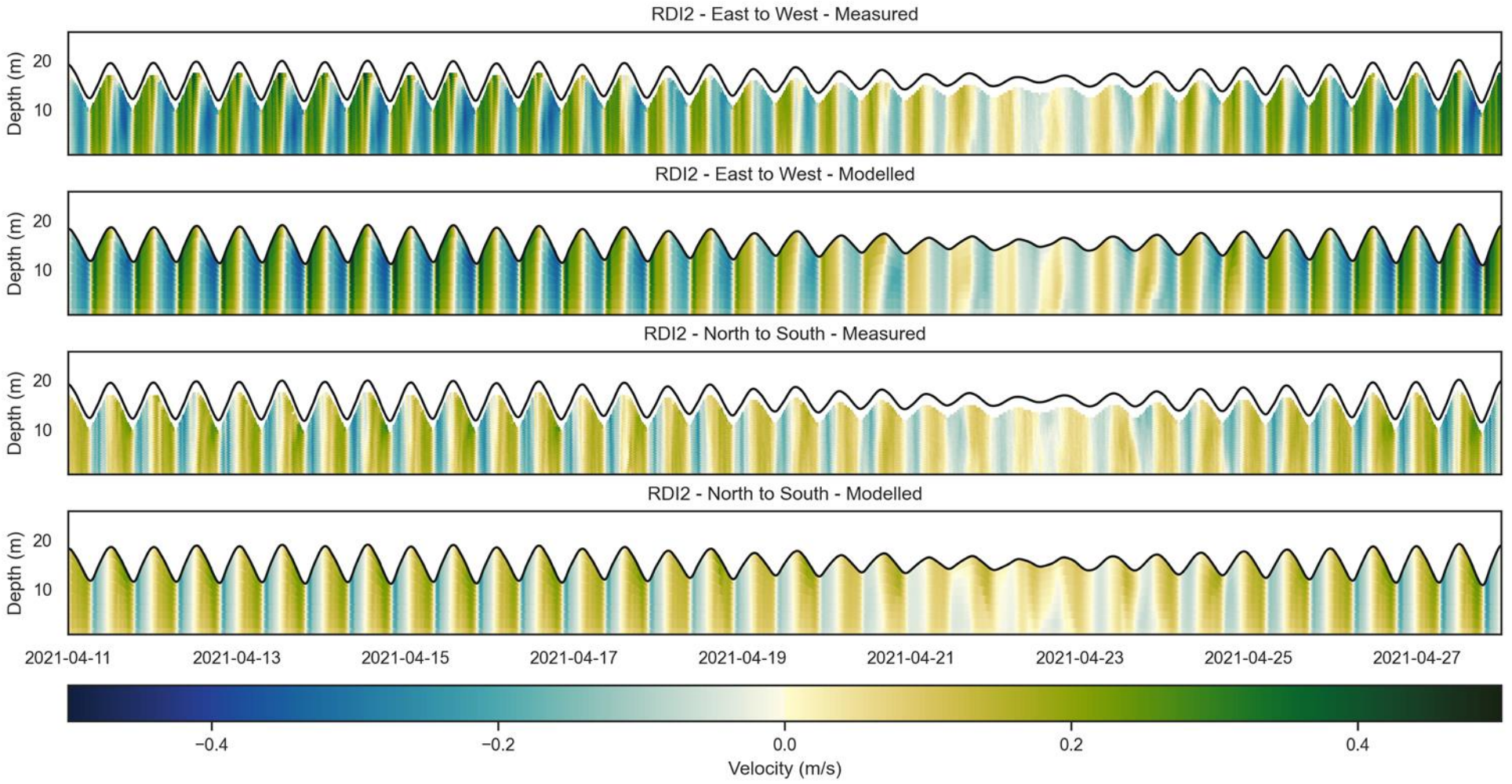


Figure 2.13 Current profiles at RD2 from April 11th to 28th 2021 showing comparison between measured and modelled east-west and north-south velocity

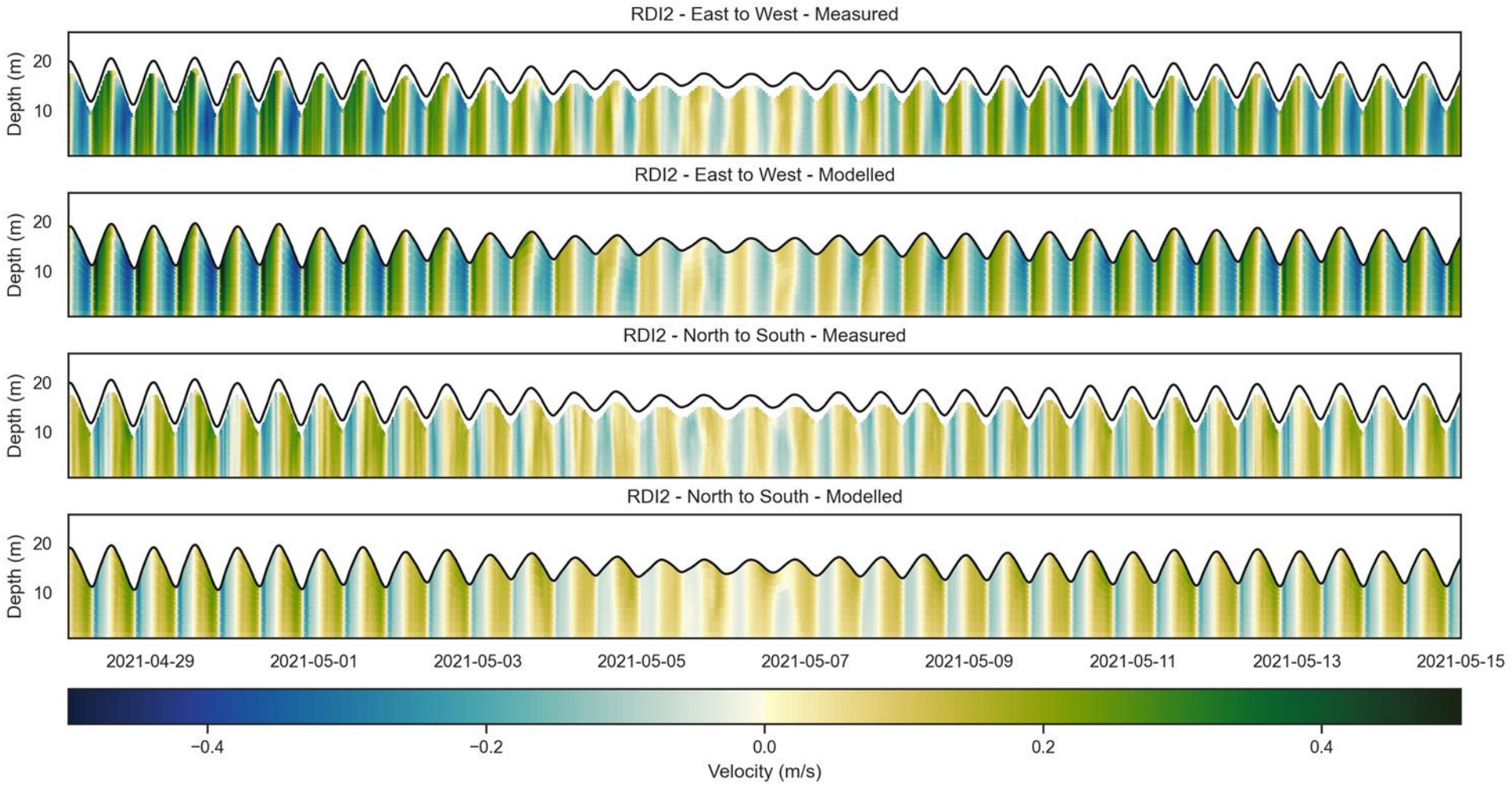


Figure 2.14 Current profiles at RD2 from April 28th to May 15th, 2021, showing comparison between measured and modelled east-west and north south velocity

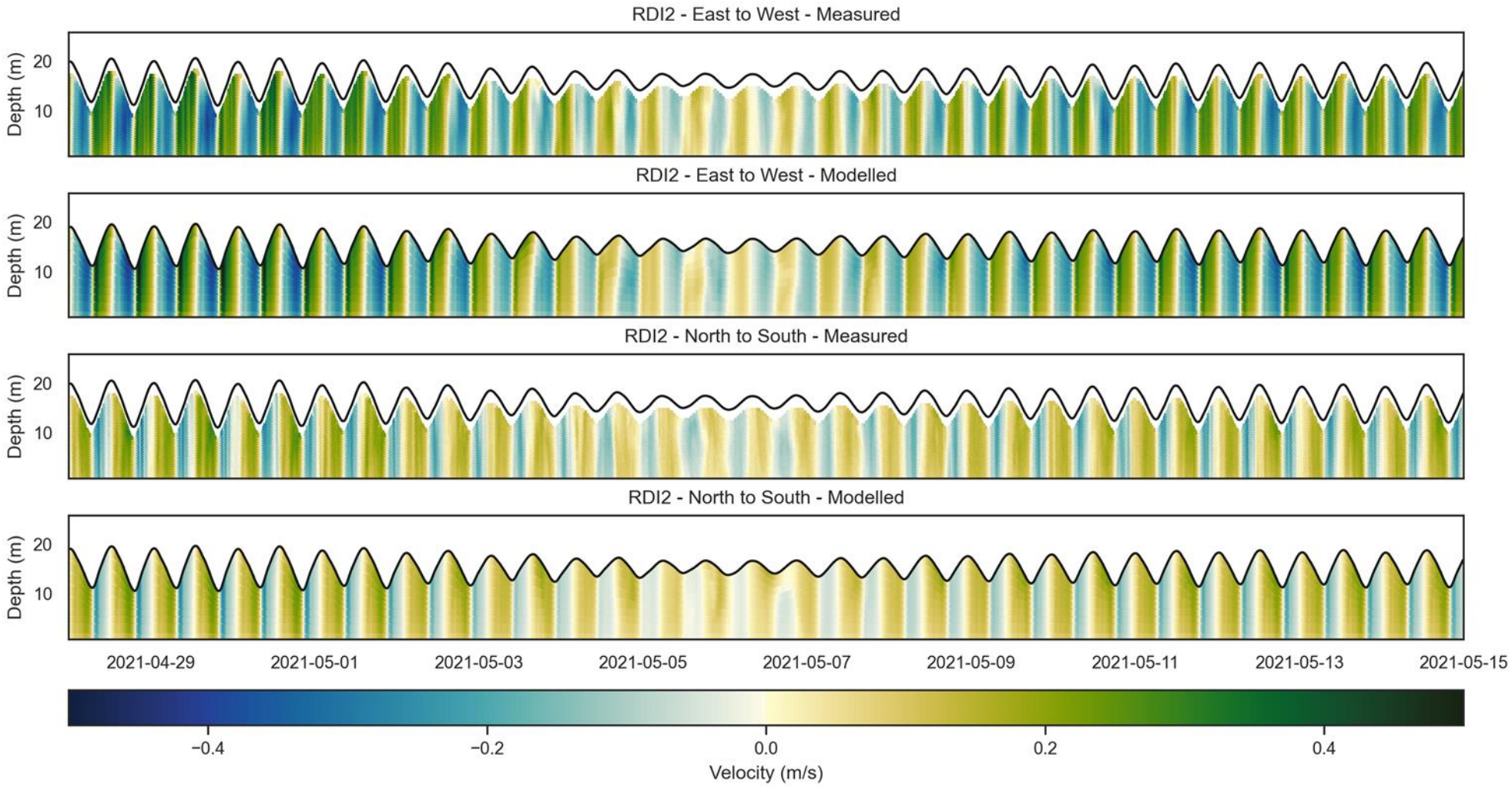


Figure 2.15 Current profiles at RD2 from April 28th to May 15th, 2021, showing comparison between measured and modelled east-west and north south velocity

### 2.5.3 Current Transects

Model predictions of current speed and direction and flow discharge were compared with measurements obtained from ADCP transects adjacent to Bayliss Island, Koolan Island and Strickland Bay. In general, the model captured a high level of accuracy in predictions for the transect data representing the vertical structure of flow as well resolving volumetric flux through key channels in the region. There were several areas however, where the model was unable to resolve fine scale flow features (e.g., Strickland Bay).

Model comparisons for transect data are provided in greater detail for each region below.

**Bayliss Island**

The model achieved a reasonably high degree of agreement with measured data, noting the following:

- The model slightly underpredicted the flow discharge, particularly at the peak flow (Figure 2.16). As bathymetry resolution and accuracy play a key role, the bathymetry around this area was finetuned to reach the optimum accuracy for the hydrodynamic model during the model calibration.
- Comparison of instantaneous velocity fields for flooding tide (Figure 2.17), high tide (Figure 2.18) and ebbing tide (Figure 2.19) show that the model resolved current speed and direction along most of the transect path reasonably well, with the greatest error shown in the northern end of the transect where bathymetry was less defined.

In general, the model is considered to resolve the flow field in the vicinity of Bayliss Island with sufficient accuracy for assessing advection and dispersion of particles and water-quality impacts. However, it should be noted that extent of dispersion in the area of Bayliss Island may be slightly underestimated, while the predicted concentrations may be slightly overestimated due to lower dilution.

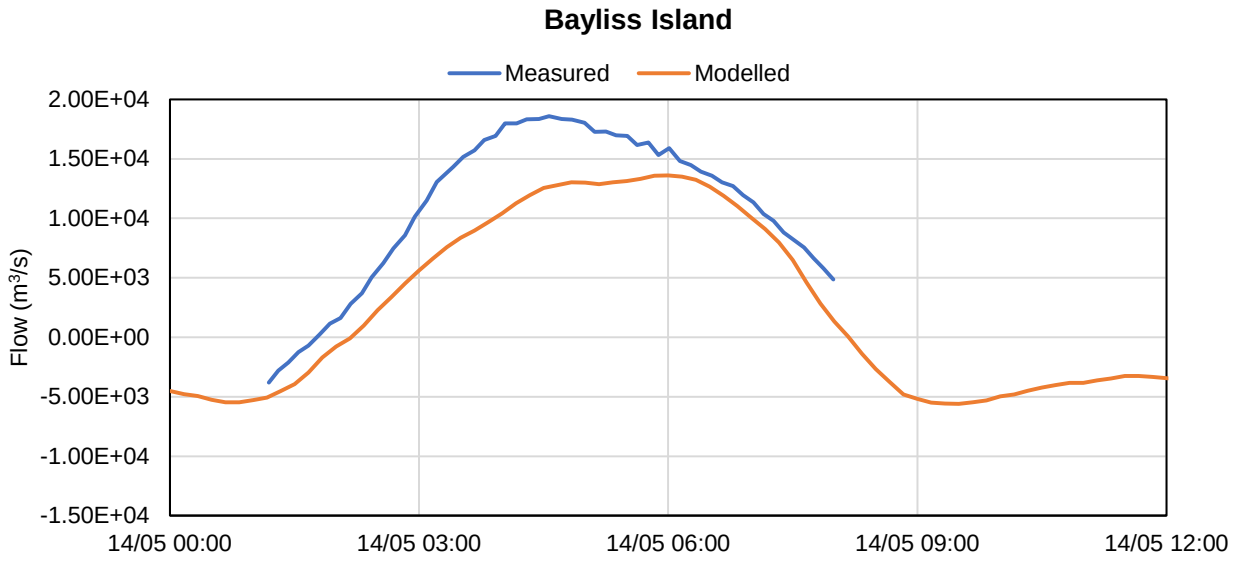


Figure 2.16 Flow discharge comparison between model and transect measurements at Bayliss Island

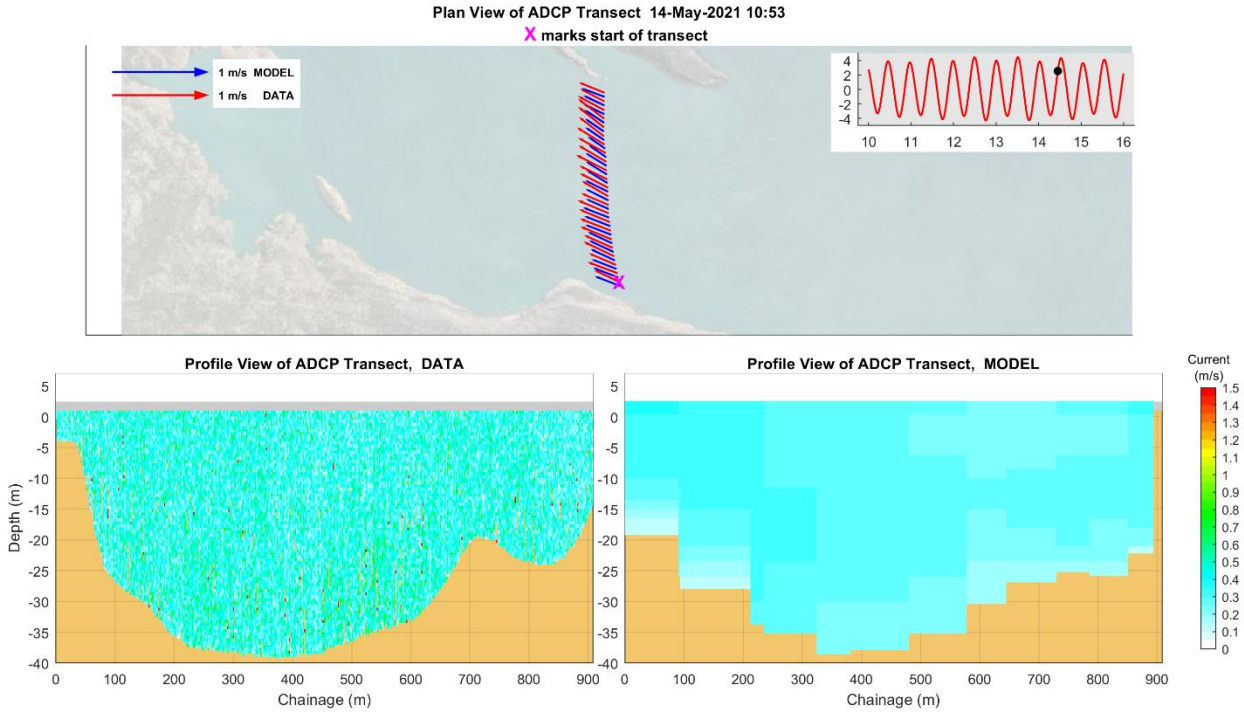


Figure 2.17 Flooding tide transect comparison at Bayliss Island (14th May 2021 10:53)

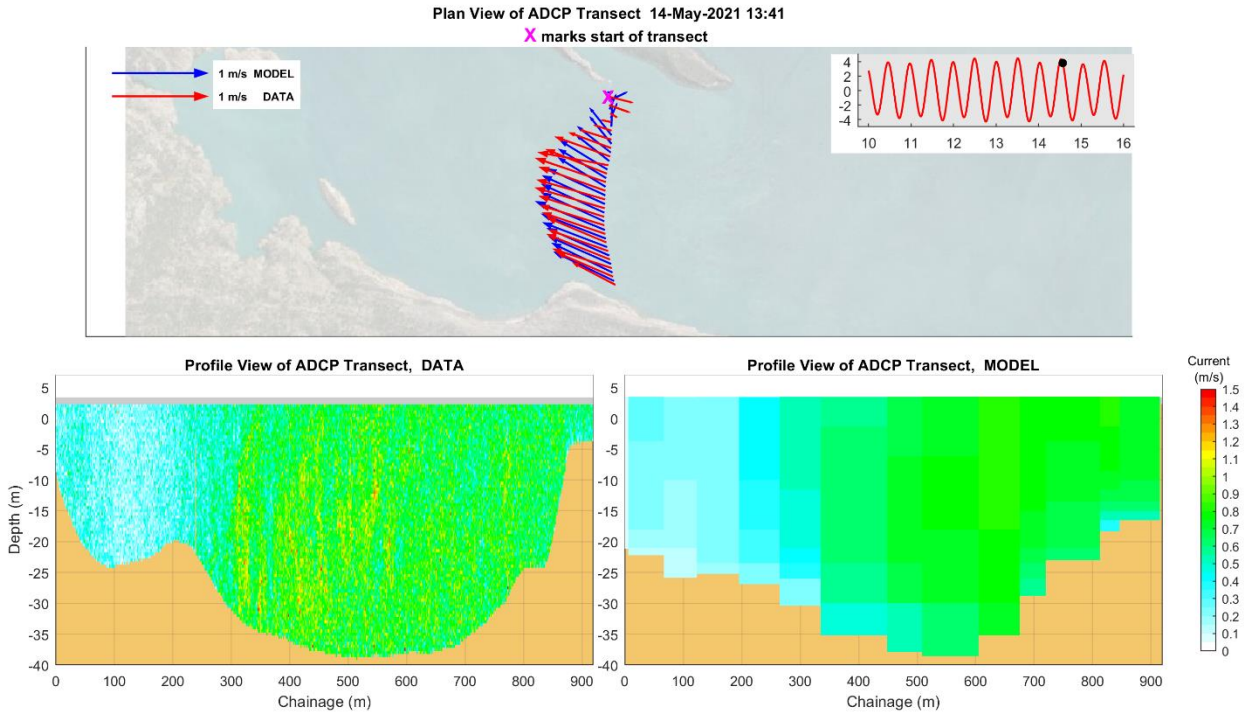


Figure 2.18 High tide transect comparison at Bayliss Island (14th May 2021 13:41)

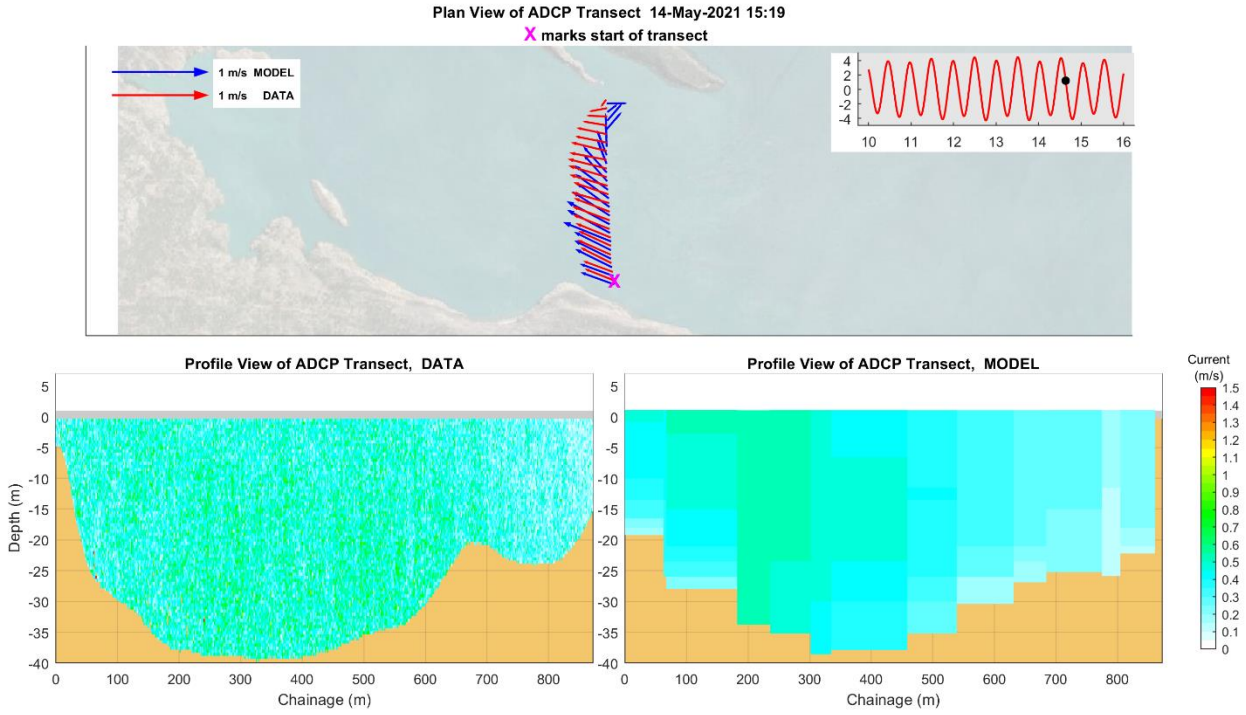


Figure 2.19 Ebbing tide transect comparison at Bayliss Island (14th May 2021 15:19)

### Koolan Island

The model shows a high degree of agreement with the measurements, noting the following:

- The predicted flow discharge is in good agreement in both phase and magnitude with measured data through the transect (Figure 2.20).
- Comparison of instantaneous velocity fields for flooding tide (Figure 2.21), high tide (Figure 2.22) and ebbing tide Figure 2.23) demonstrate that the model resolved the current speed and direction along most part of the transect reasonably well, except at the two ends where the model slightly underestimated the current speed. The underestimation at the ends has little to no impact on the dispersion and dilution of material in the vicinity of Koolan Island because these areas are generally shallow.

In general, the model is considered to resolve the area in the channel near Koolan Island with sufficient accuracy for assessing advection and dispersion of particles and water-quality impacts.

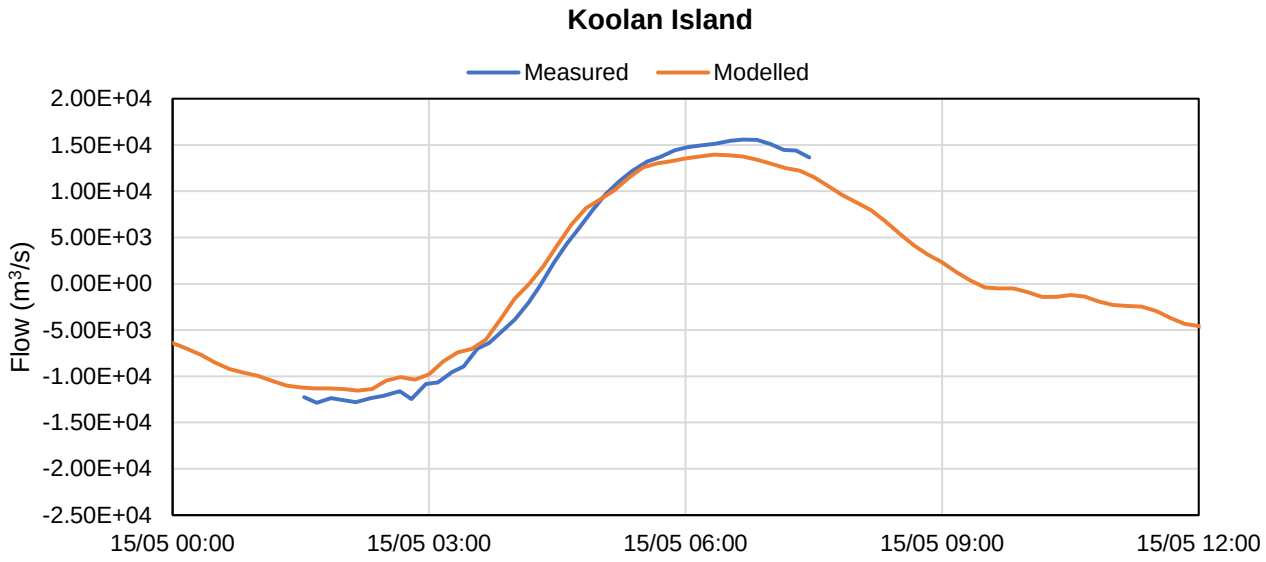


Figure 2.20 Flow discharge comparison between the model and transect measurements at Koolan Island

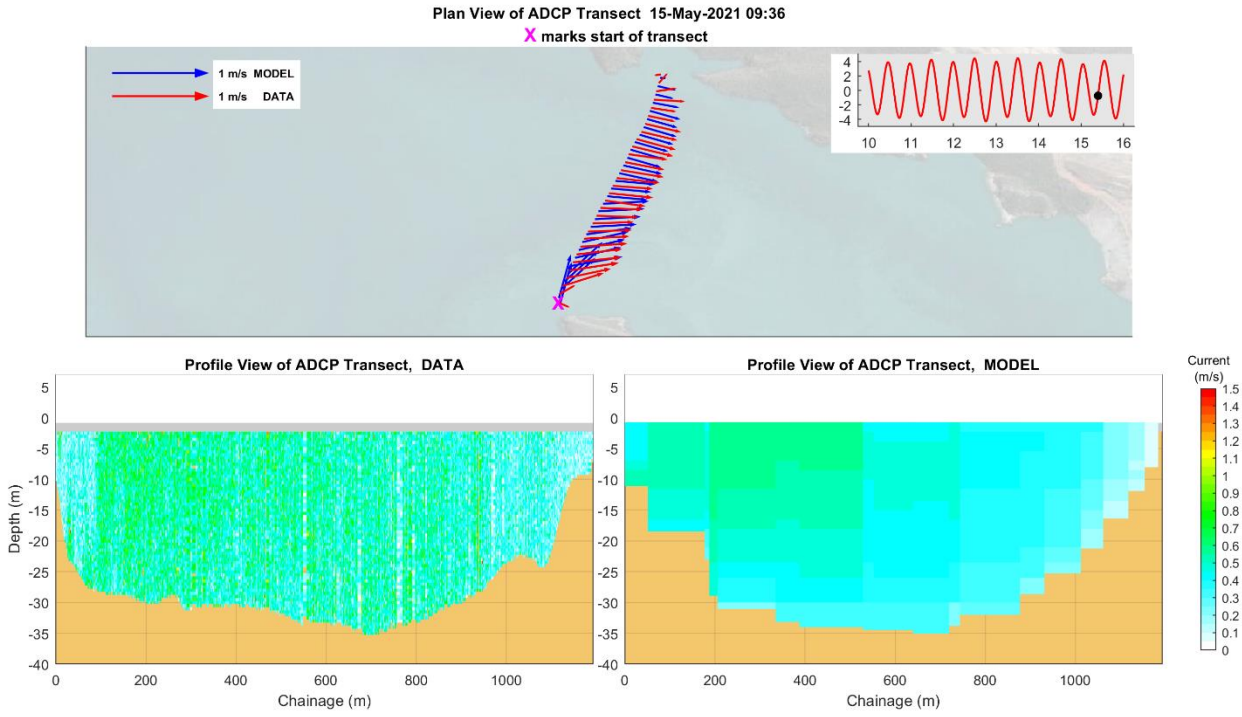


Figure 2.21 Flooding tide transect comparison at Koolan Island (15th May 2021 09:36)

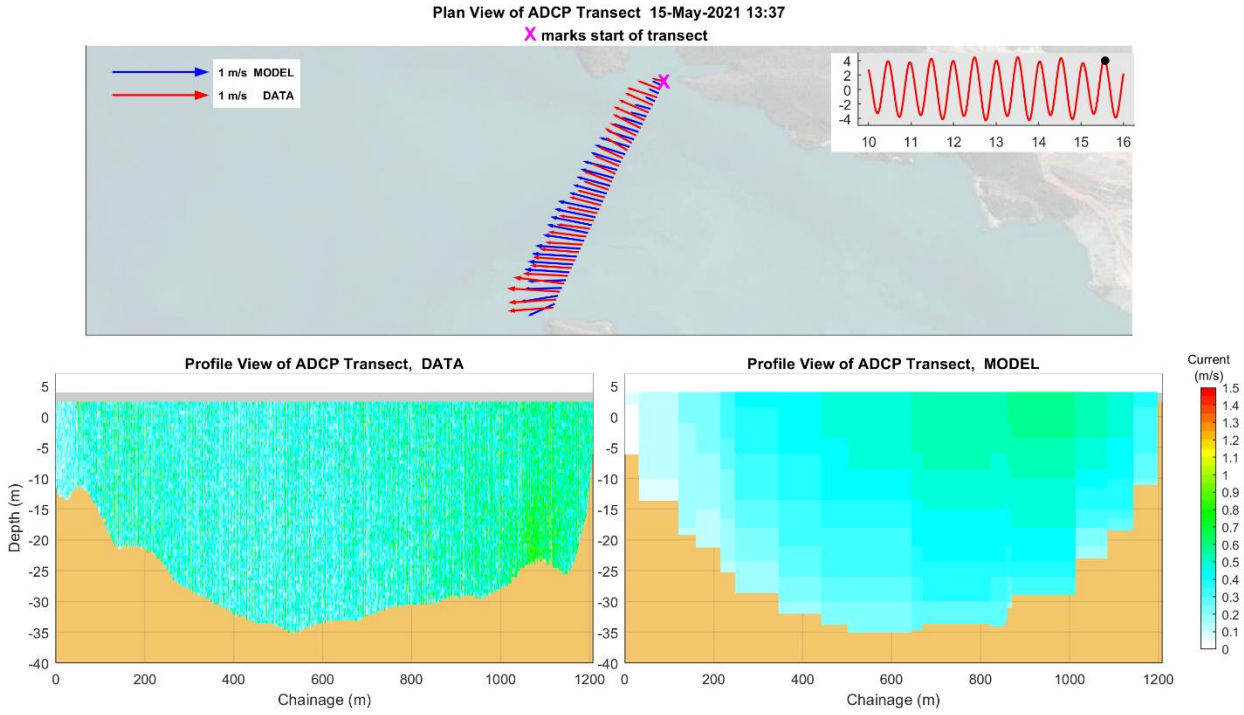


Figure 2.22 High tide transect comparison at Koolan Island (15th May 2021 13:37)

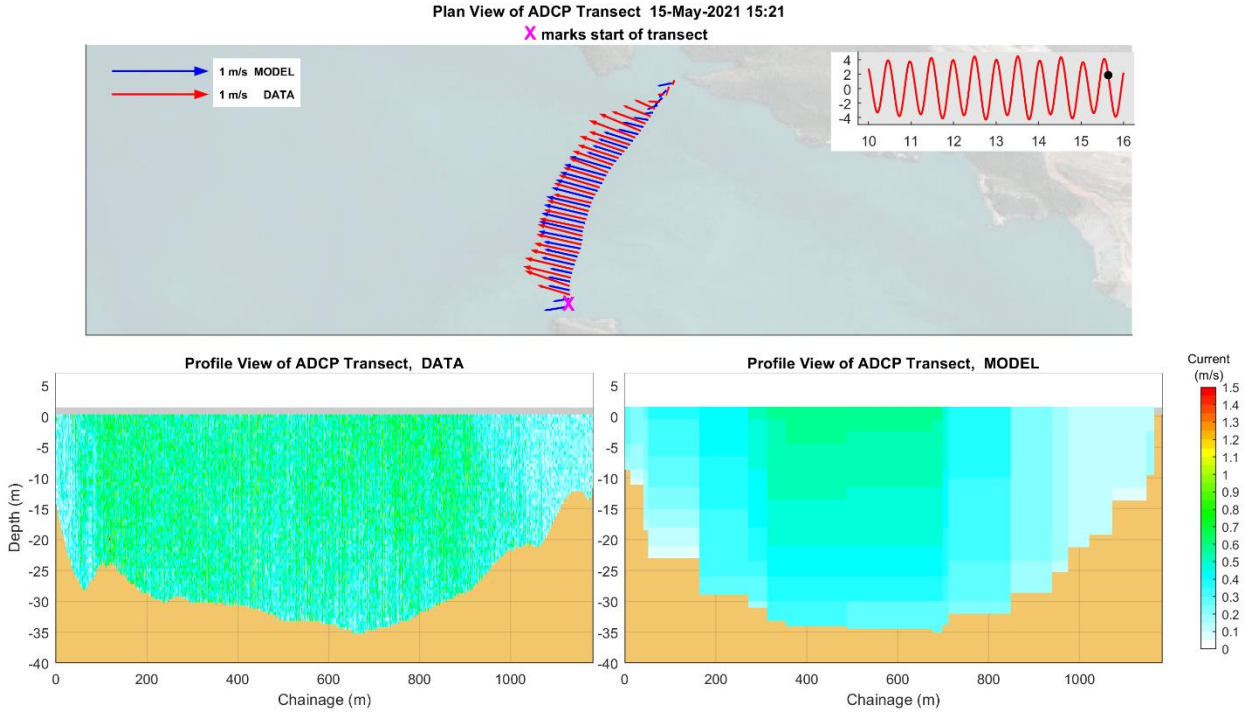

Figure 2.23 Ebbing tide transect comparison at Koolan Island (15th May 2021 15:21)

### Strickland Bay

The model showed a reasonably good level of agreement with measurements, noting the following:

- The observed flow discharge was closely replicated by the model in Strickland Bay with good agreement in magnitude and a slight phase difference of less than 1 hour (Figure 2.24).
- Comparison of instantaneous velocity fields for flooding tide (Figure 2.25), high tide (Figure 2.26) and ebbing tide (Figure 2.27) demonstrate a good match to measurements across the entire transect. However, the model did not resolve the local peak flows across the transect (e.g., in the deep channel at the northern end of the transect).

The model appears to well represent this area in terms of overall current speed, direction, and total volumetric flow; however, it is noted that the inability of the model to resolve small-scale features (e.g., the sharp gradient in flow in the deep channel) may result in slightly underestimated footprints (and overestimated magnitudes) of dispersed particles within the vicinity of Strickland Bay.

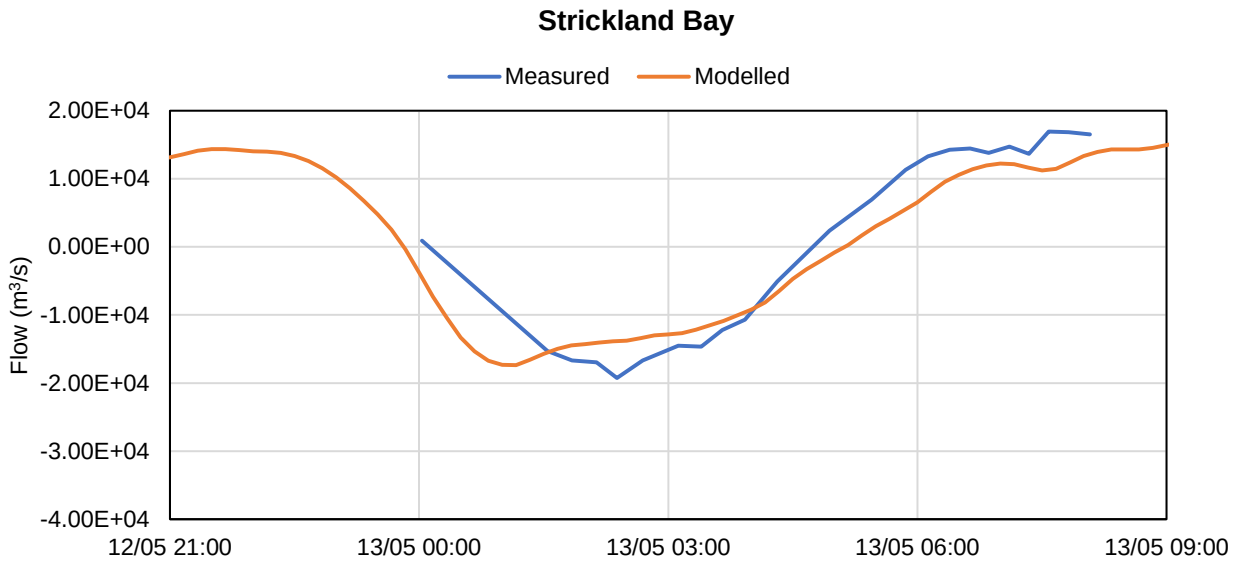


Figure 2.24 Flow discharge comparison between the model and transect measurements at Strickland Bay

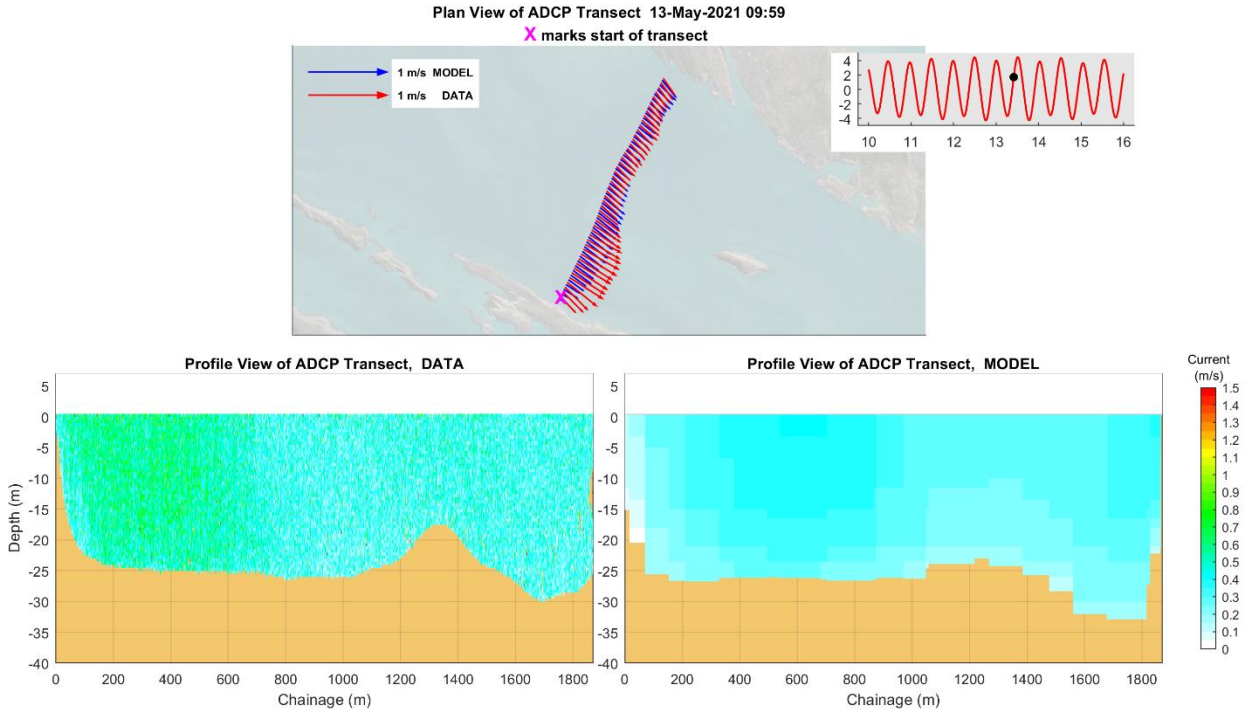


Figure 2.25 Flooding tide transect comparison at Strickland Bay (13th May 2021 09:59)

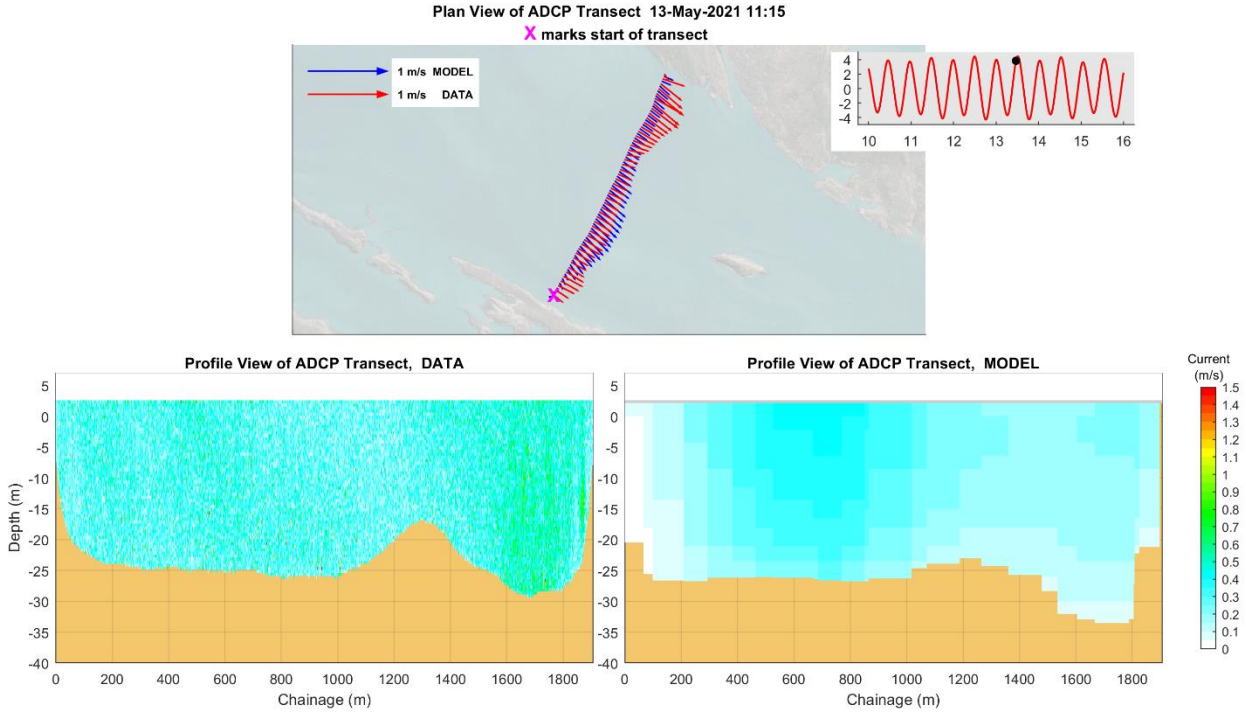


Figure 2.26 High tide transect comparison at Strickland Bay (13th May 2021 11:15)

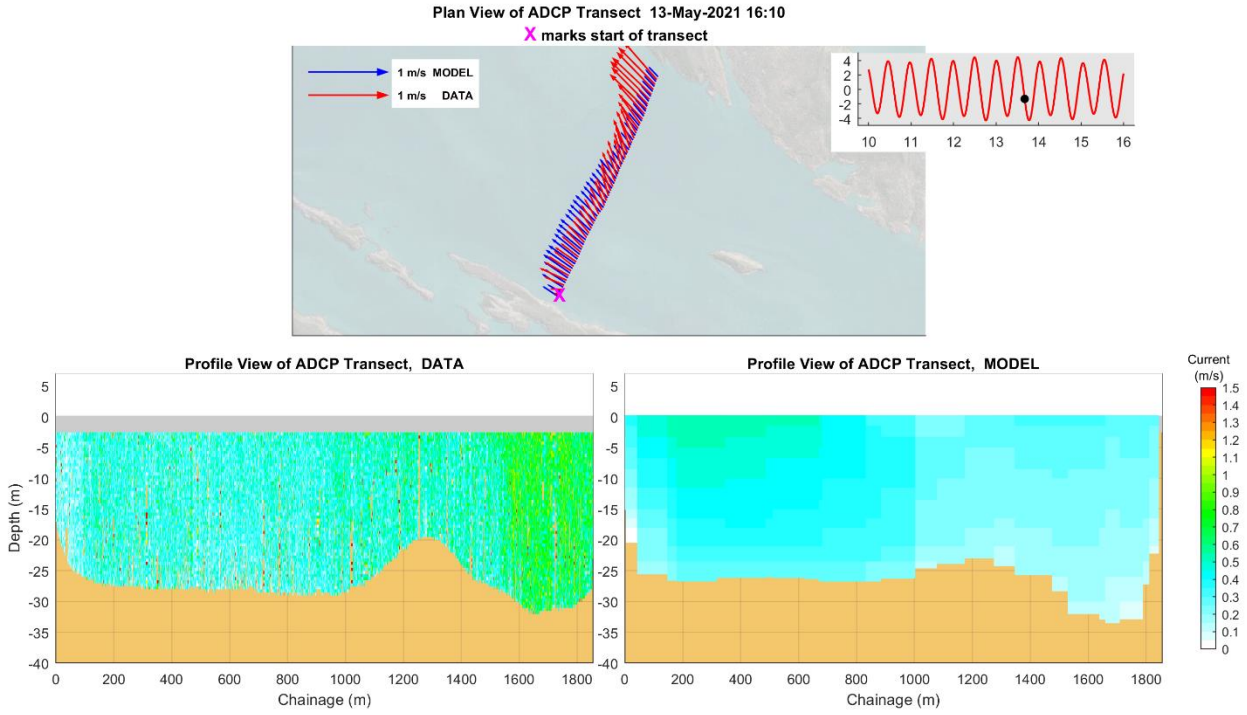


Figure 2.27 Ebbing tide transect comparison at Strickland Bay (13th May 2021 16:10)

## 2.6 Temperature

A reliable temperature calibration is of primary importance to the water quality model, as temperature has a controlling effect on the rate of key biogeochemical processes. Visual and quantitative comparisons between modelled and measured depth averaged temperature for RDI1 and RDI2 are shown in Figure 2.28 and Figure 2.29, with model performance metrics listed in Table 2.5.

In general, the model closely replicated the depth-averaged temperatures in both locations, with slight overprediction (<0.5$^{o}$C) recorded at RDI2. The model reproduced both the cooling phase observed from 17$^{th}$ – 25$^{th}$ of April and following heating phase. Furthermore, the daily variation in the depth-averaged temperature at both locations was closely reproduced by the model. Modelled temperatures showed a high IOA (0.88) with measurements from both locations. The model predicted temperatures fell within 0.5$^{o}$C of the measured data with RMSE < 0.31$^{o}$C and MAE < 0.27$^{o}$C (Table 2.5). The modelled surface and bottom temperature were not significantly different in magnitude indicating a mixed water column during the comparison period.

Table 2.5 Temperature validation scores

| Station | IOA | RMSE ($^{o}$C) | MAE ($^{o}$C) |
|---|---|---|---|
| RDI1 | 0.88 | 0.19 | 0.16 |
| RDI2 | 0.88 | 0.31 | 0.27 |

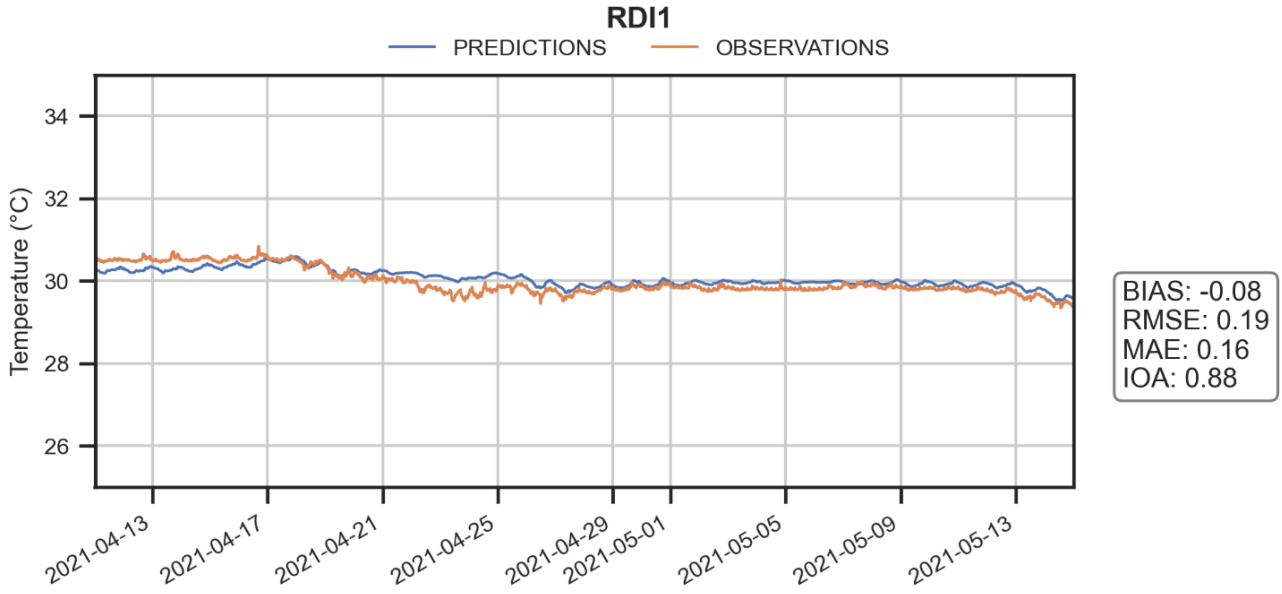


Figure 2.28 Modelled and measured Temperature comparison at RDI1

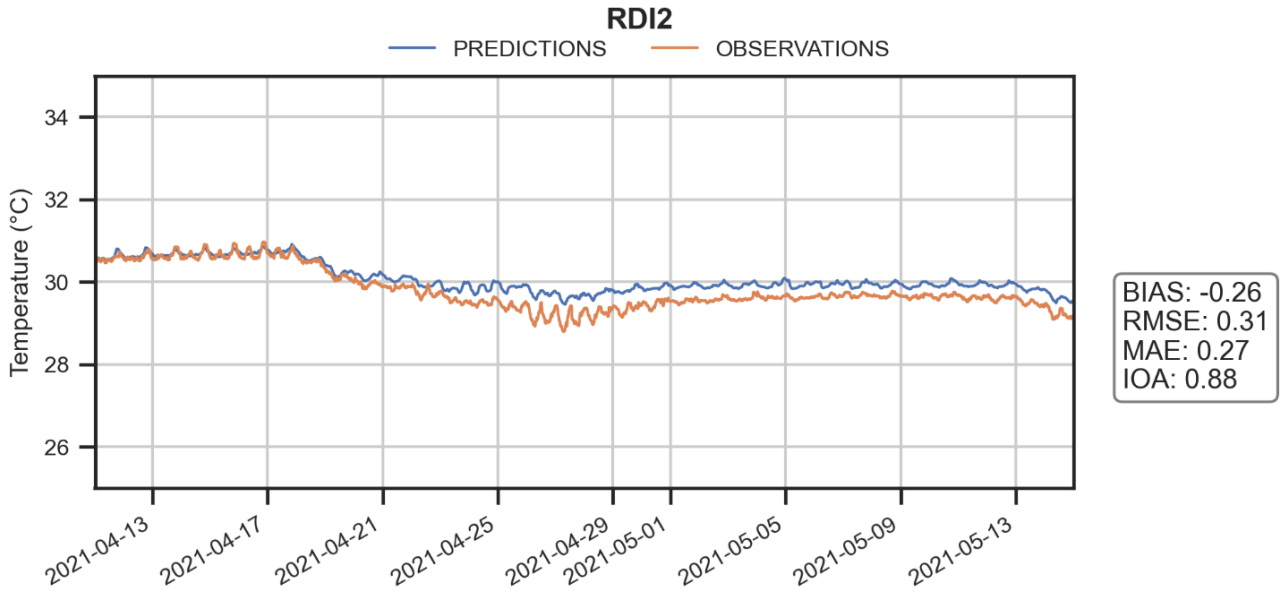


Figure 2.29 Modelled and measured Temperature comparison at RDI1

# 3 Water quality model calibration

Dynamically linked to the hydrodynamic model, the water quality model was used to simulate transport and internal dynamics of water quality variables and compare baseline conditions with impact of the proposed farm expansion plans. The EIA requires simulation of projected increases in nutrients and primary productivity to determine a sustainable carrying capacity in the proposed sites. The water quality calibration was thus focussed on establishing a representative model baseline for nitrogen, phosphorus and chlorophyll-a concentrations. The model calibration process was achieved by adjusting model boundary conditions from ocean upwelling and riverine flows, mineralisation of organic nutrients, phytoplankton growth rates and sediment fluxes to achieve best fit to spatial and seasonal gradients in the observed data.

## 3.1 Field observations

Monitoring data provided by Tassal and used for model calibration were collected at 28 stations within the Buccaneer Archipelago representing a range of inner near coastal areas, proposed aquaculture sites and outer boundary sites (Figure 3.1). While the boundary stations were located some distance from the model's open ocean boundary, they were used to represent the offshore water quality concentrations. Grab samples were taken at all stations approximately twice a month from February to April 2021 (representing wet season conditions) and June to August 2021 (representing dry season conditions) for the following key environmental variables:

- Ammonium (NH4), nitrate and nitrite (NOx), total nitrogen (TN)
- Filterable reactive phosphorus (FRP) and total phosphorus (TP)
- Chlorophyll-*a* (Chl-a).

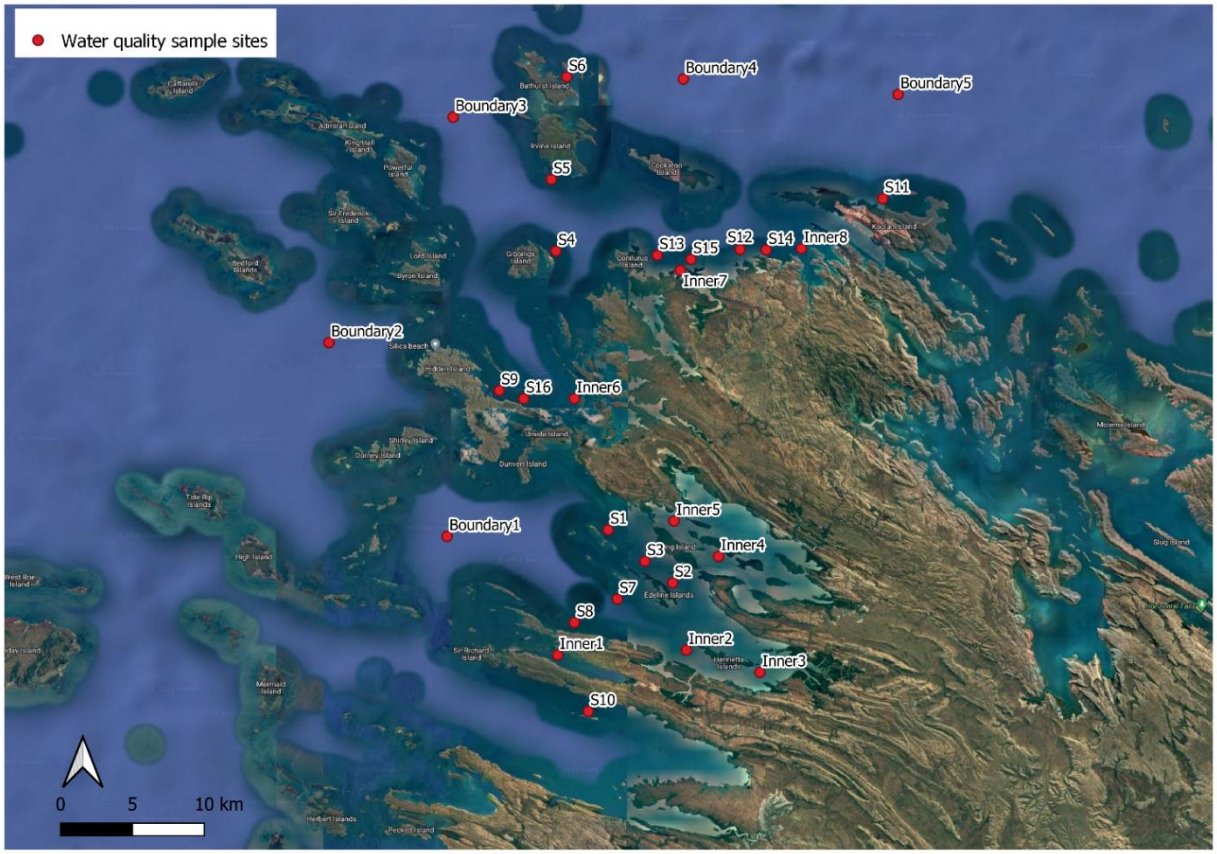


Figure 3.1 Map showing water quality sampling stations used in model verification

## 3.2 Performance criteria

Due to the limited size of observations necessary for statistical fit comparisons, the model outputs were compared with observed concentrations through visual observations of timeseries and annual medians over the two sampling periods representing the dry and wet season.

## 3.3 Model calibration

The water quality samples taken during the monitoring program reflected the oligotrophic status of the Buccaneer Archipelago study area, with low nutrient and chlorophyll-*a* concentrations that were often below the limits of detection. There is also little in the way of temporal variability and, therefore, no clear system dynamics to calibrate the model to. As such, the calibration process was reduced to one of 'verification', which simply compared simulated water quality concentrations to observations, without the need for changes to water quality parameter sets. This section provides those comparisons for the key variables.

### 3.3.1 Chlorophyll-a (Chl-a)

For most of the simulated period, observed concentrations of chlorophyll-*a* were relatively low, less than 1.5 µg/L. The model was parameterised to reproduce the consistently low values observed in both wet and dry seasons (Figure 3.2 through to Figure 3.4).

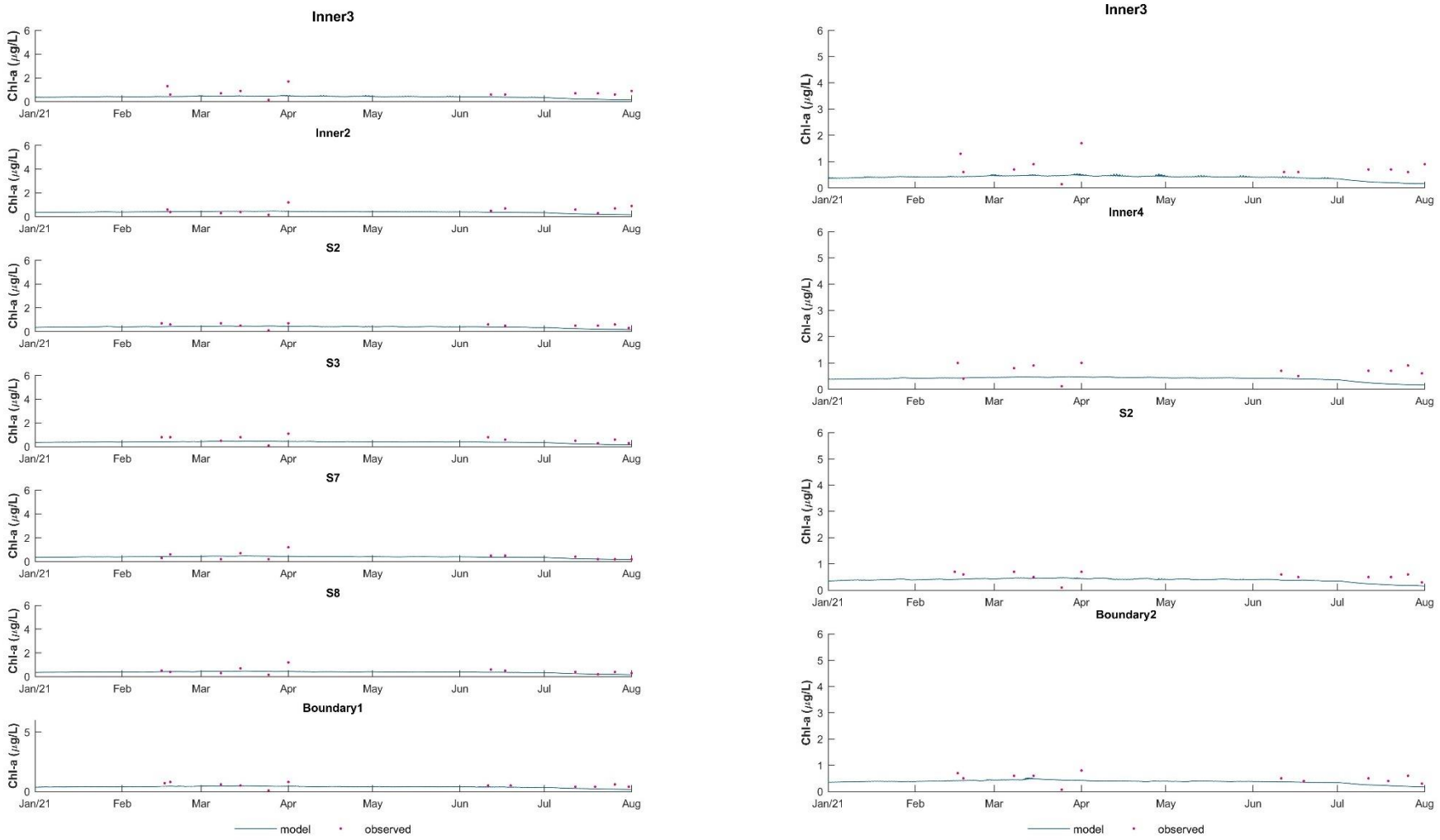


Figure 3.2 Time-series of Chl-*a* at the water quality stations between Inner 3 (neashore) and Boundary 1/Boundary 2 (Offshore)

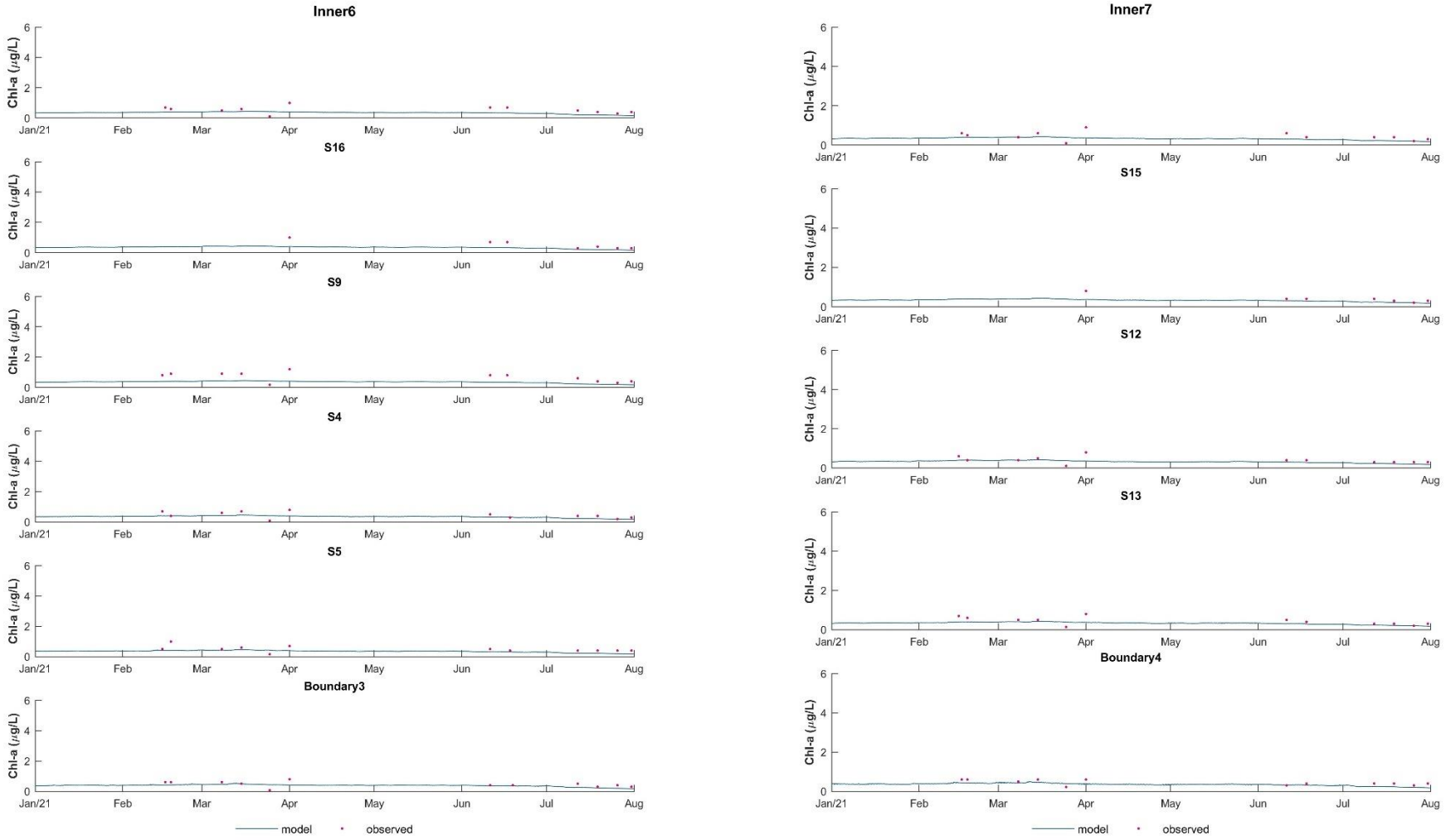


Figure 3.3 Time-series of Chl-a at the water quality stations between Inner 6/Inner 7 (neashore) and Boundary 3/Boundary 4 (Offshore)

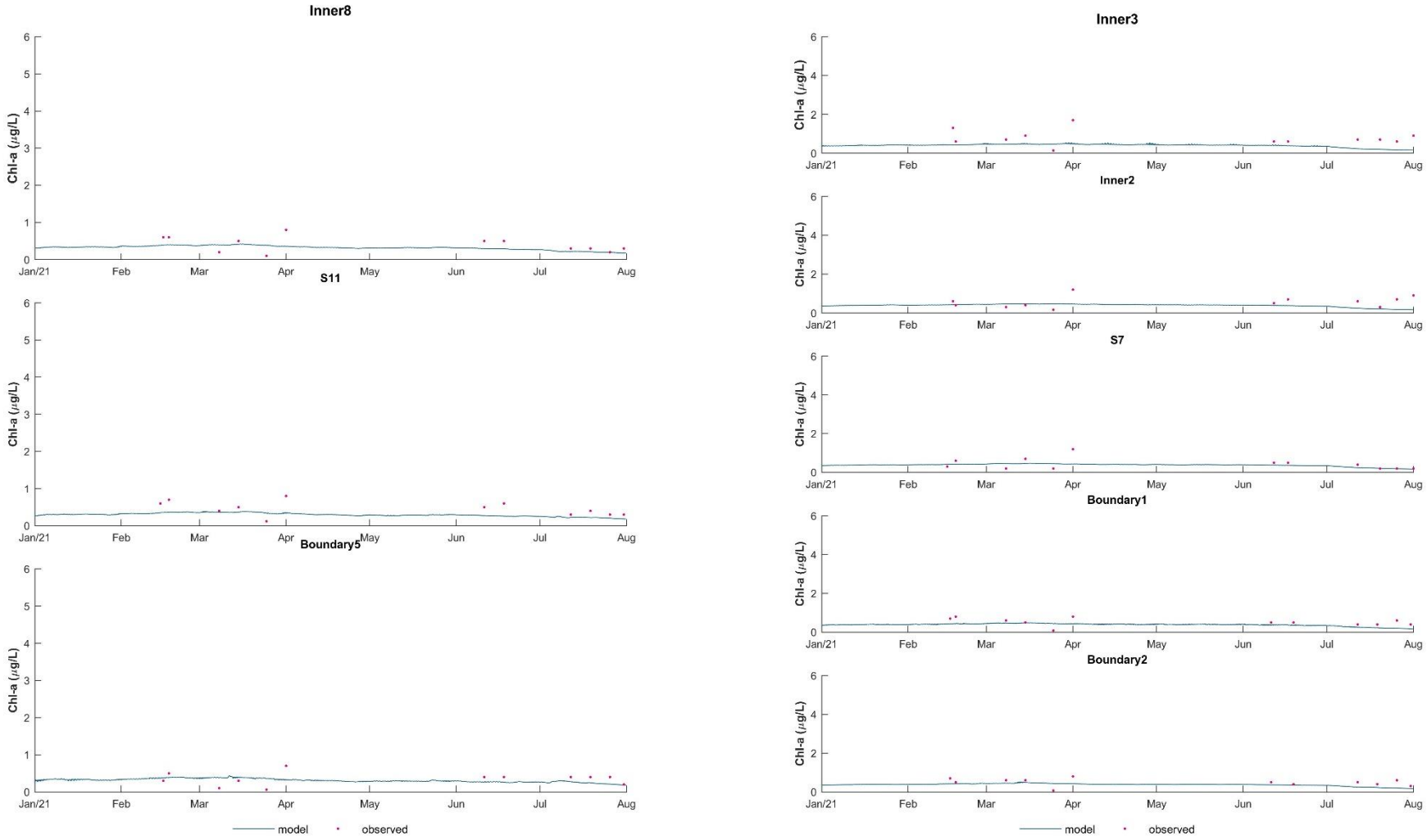


Figure 3.4 Time-series of Chl-a at the water quality stations between Inner 8/Inner 3 (neashore) and Boundary 5/Boundary 2 (Offshore)

### 3.3.2 Nitrogen

Measured concentrations of NH4 and NOx for both wet and dry sampling periods were generally low (<0.005 mg/L) or below limit of detection, so time series calibration focusses on matching observations of total nitrogen (TN). Modelled TN concentrations did not vary significantly during the simulation period in general agreement with measured data including slight reduction during the dry season (Figure 3.5 to Figure 3.6).

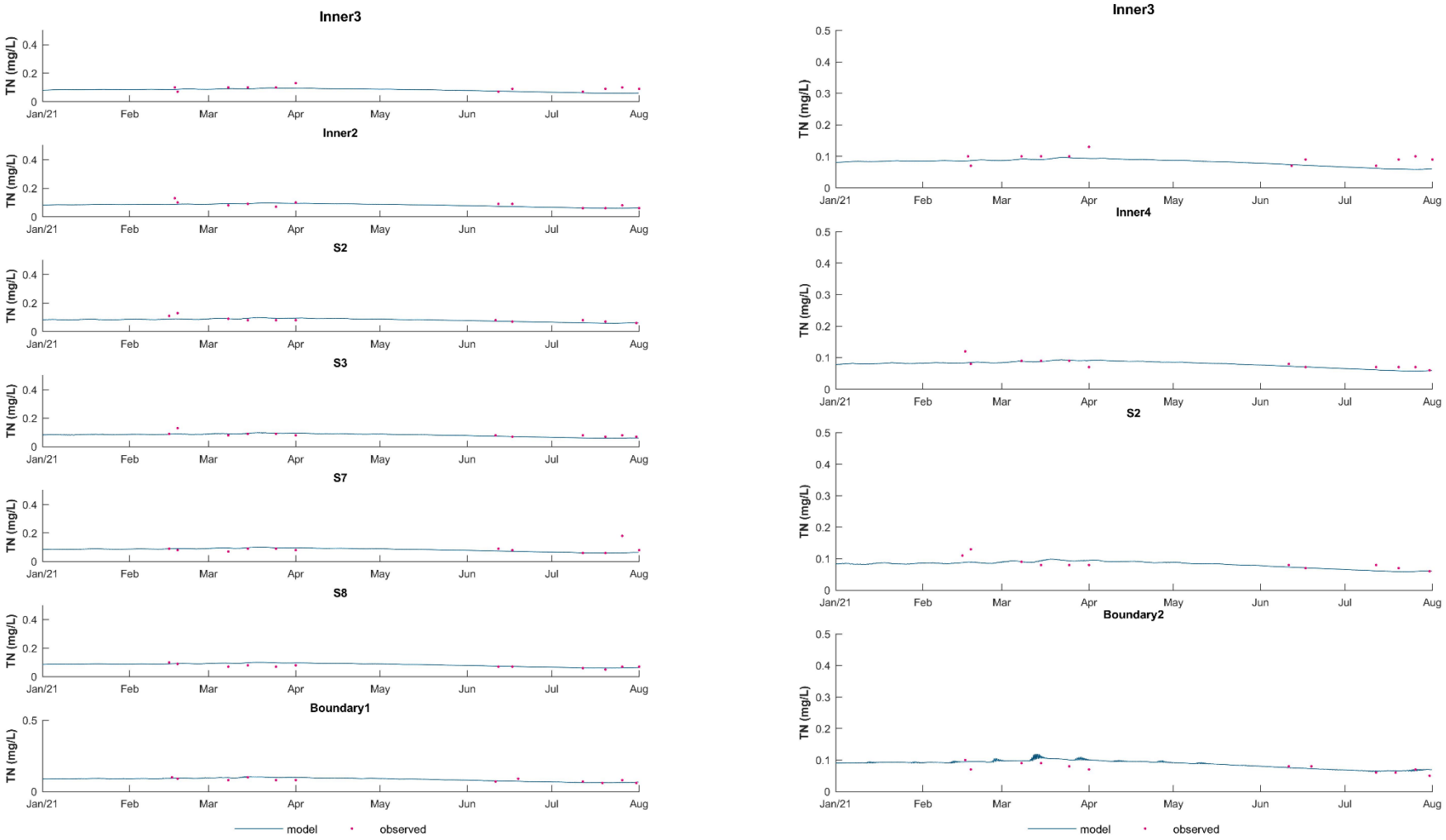


Figure 3.5 Time-series of TN at the water quality stations between Inner 3 (neashore) and Boundary 1/Boundary 2 (Offshore)

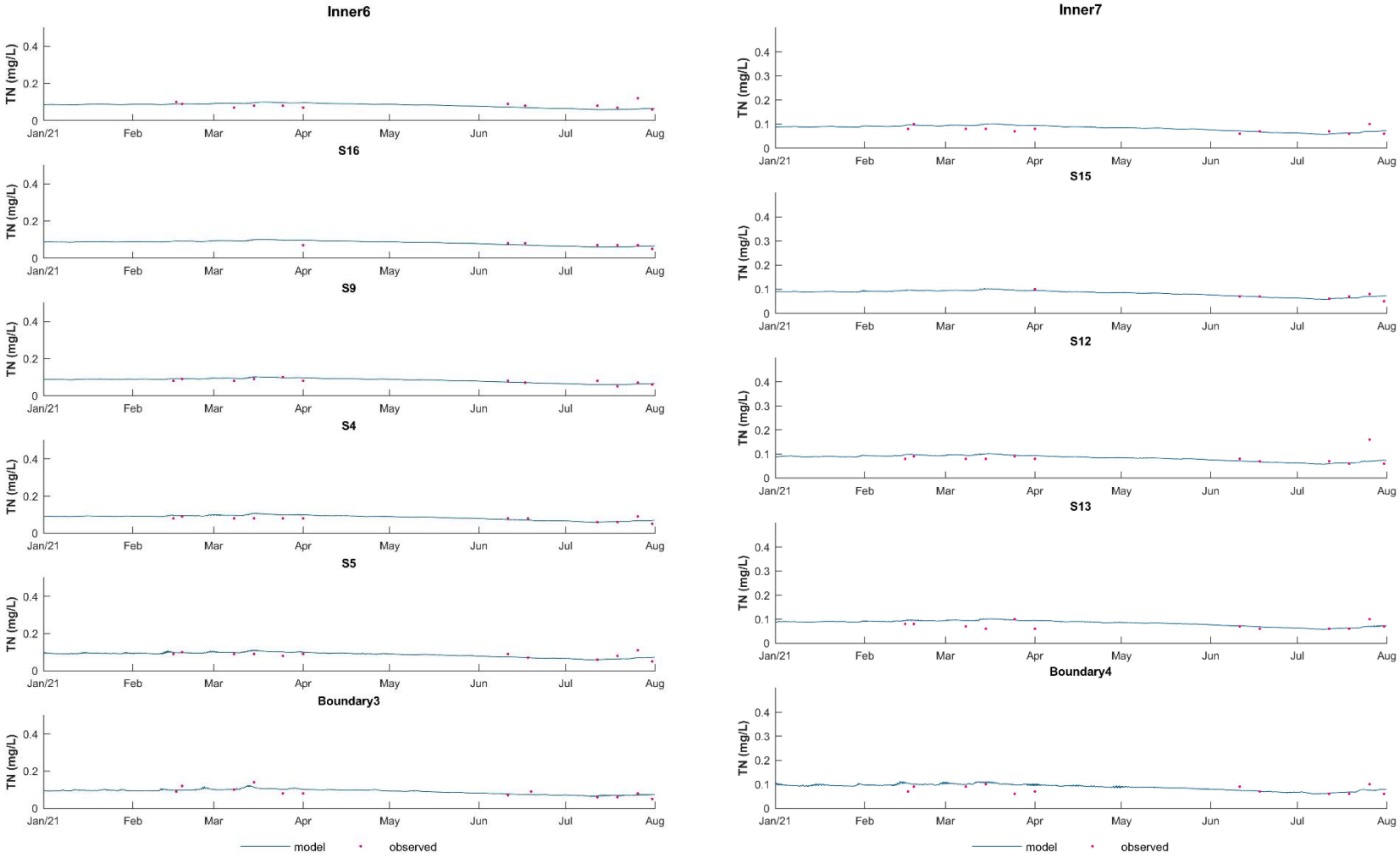


Figure 3.6 Time-series of TN at the water quality stations between Inner 6/Inner 7 (neashore) and Boundary 3/Boundary 4 (Offshore)

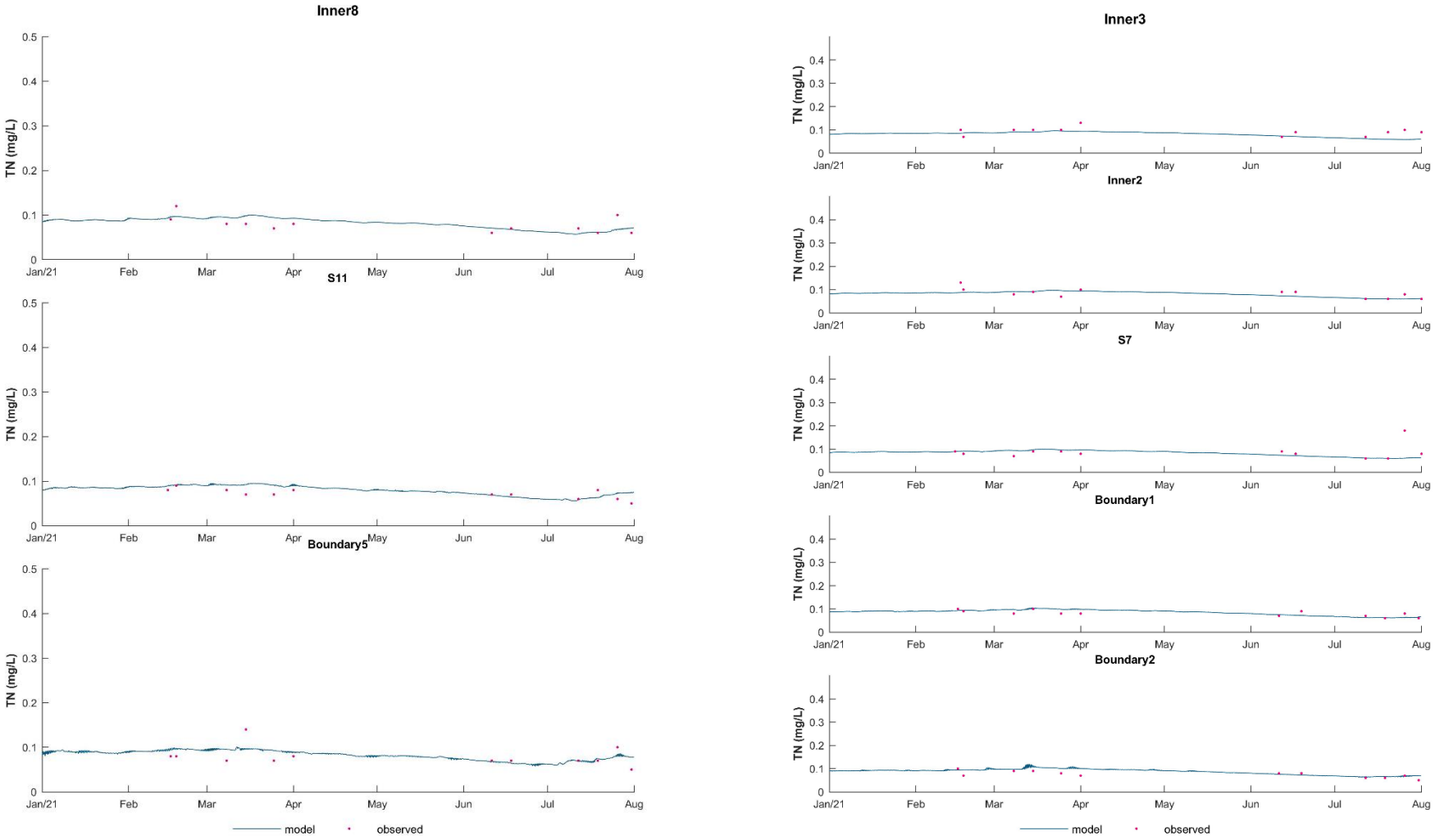


Figure 3.7 Time-series of TN at the water quality stations between Inner 8/Inner 3 (neashore) and Boundary 5/Boundary 2 (Offshore)

### 3.3.3 Filterable Reactive Phosphate (FRP) and Total Phosphorus (TP)

Comparisons of simulated and observed FRP are presented in Figure 3.8 through to Figure 3.10. Both predicted and measured concentrations of FRP and TP were typically low < 0.02 mg/L. The model over predicted FRP concentrations throughout the model domain although neither model nor measured concentrations varied substantially during the calibration period.

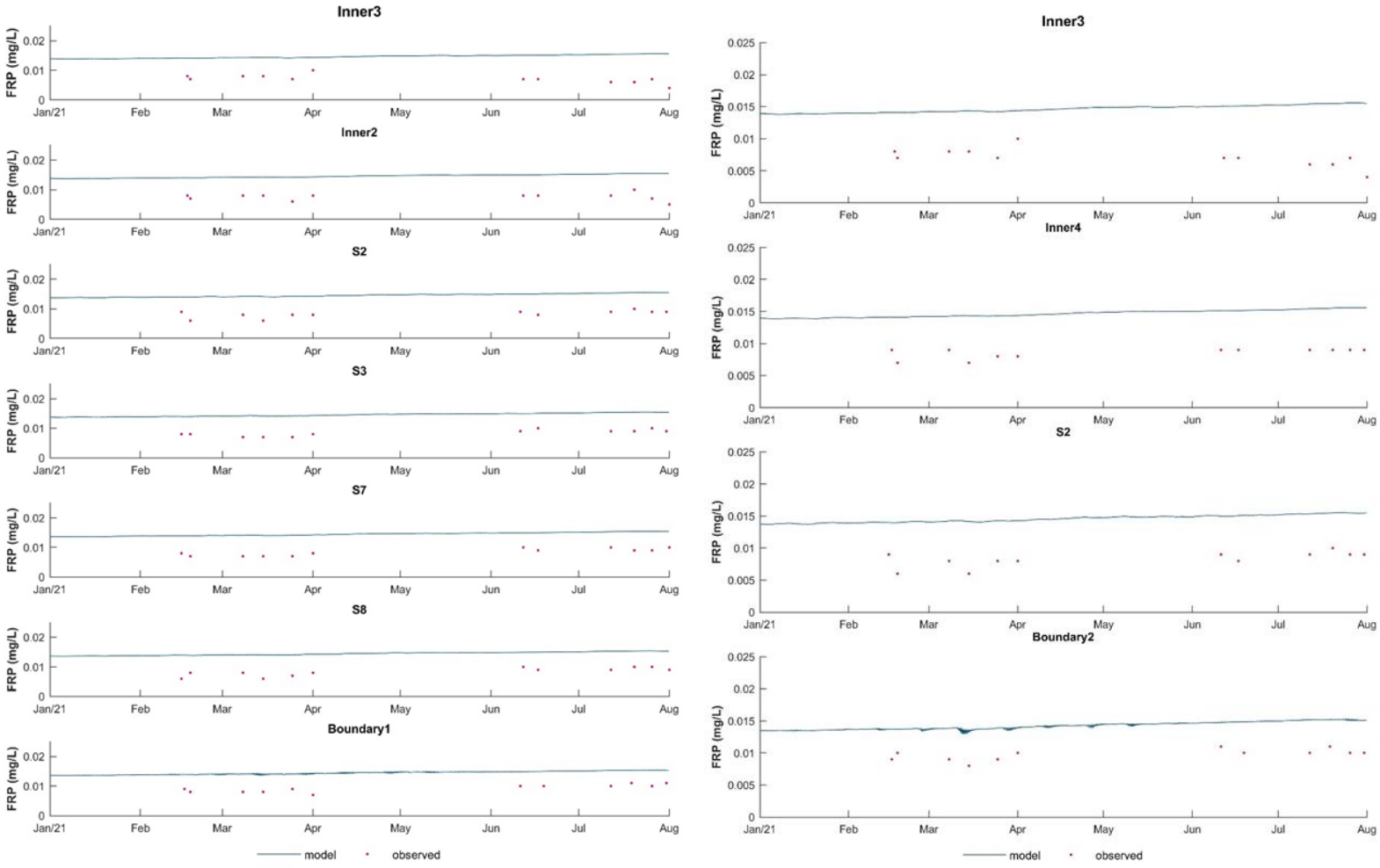


Figure 3.8 Time seres of FRP at the water quality stations between  Inner 3 (neashore) and Boundary 1/Boundary 2 (Offshore)

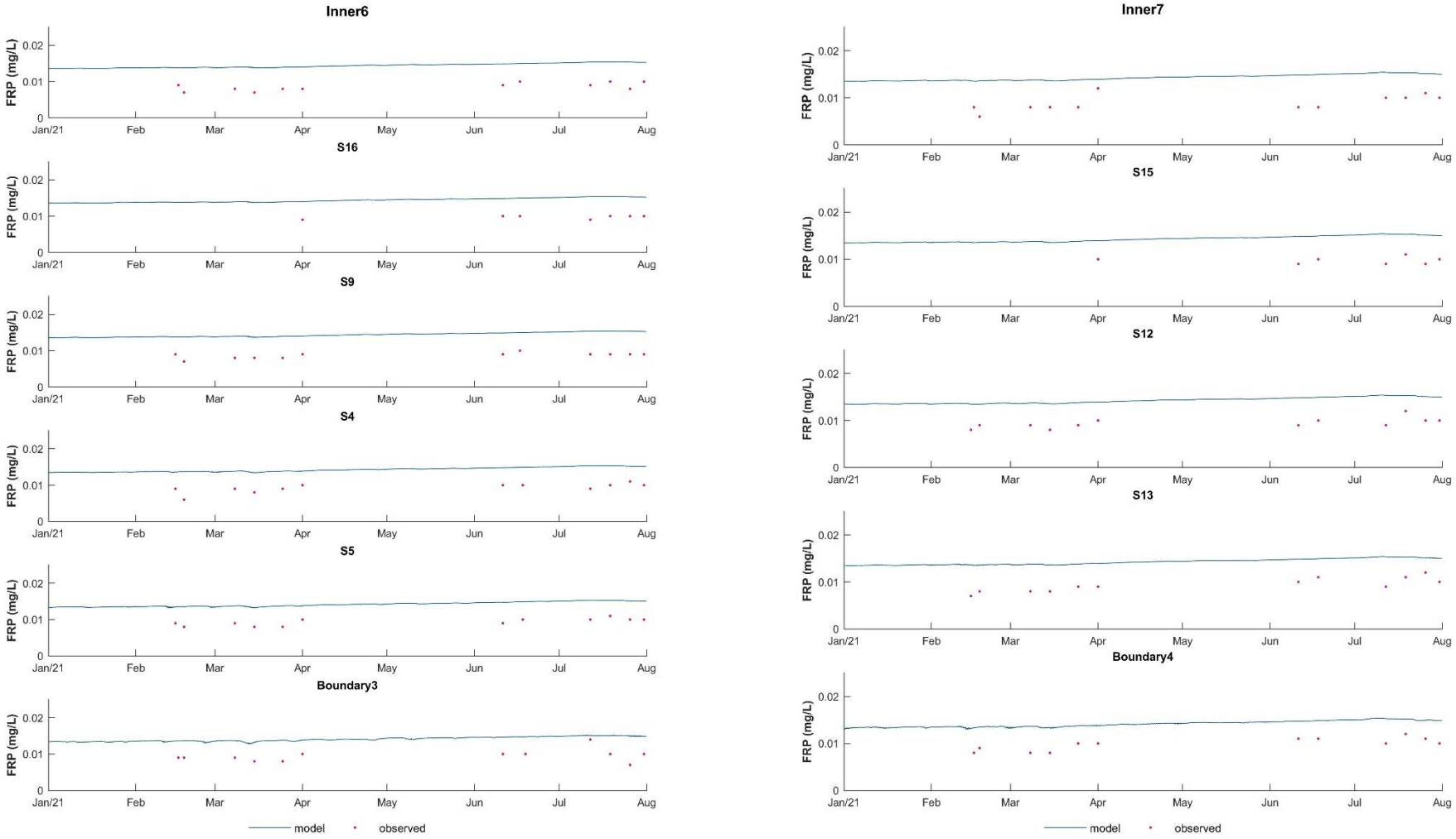


Figure 3.9 Time-series of FRP at the water quality stations between Inner 6/Inner 7 (neashore) and Boundary 3/Boundary 4 (Offshore)

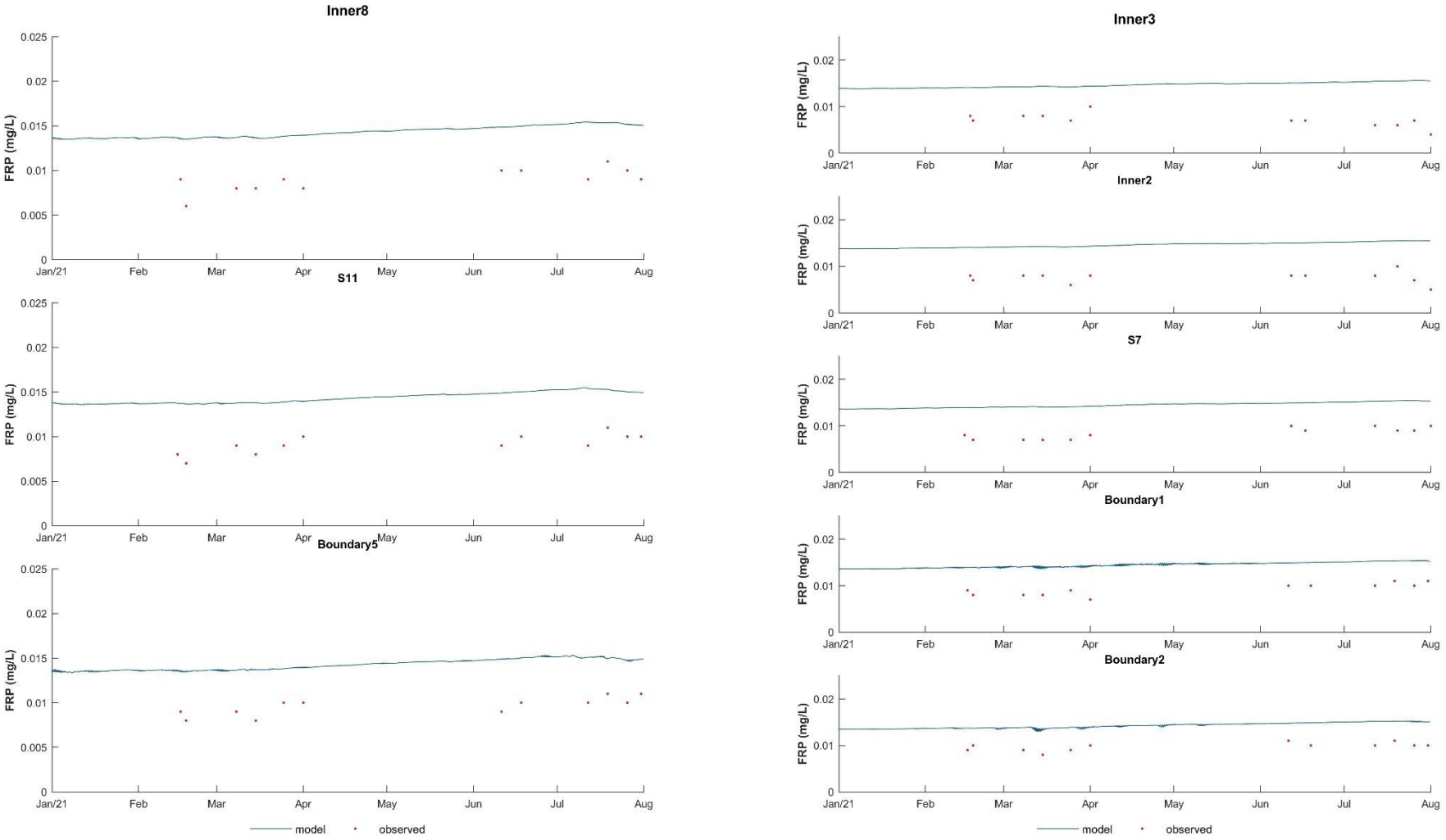


Figure 3.10 Time-series of FRP at the water quality stations between Inner 8/Inner 3 (neashore) and Boundary 5/Boundary 2 (Offshore)

### 3.3.4 Quantile-quantile median comparisons

Comparison of model medians against measured quantile-quantile and medians were used to verify that the water quality model was representing observed spatial trends in the Buccaneer Archipelago (Figure 3.11 and Figure 3.12).

- For Chl-a, model predictions were consistent with observations and the bioavailability of nutrients in the water column, simulating a decrease in the median concentration of Chl-a towards the offshore locations.
- The observed medians for NH4, NOx and TN concentrations were consistently low, <0.005, <0.003 and <0.12 mg/L, respectively. Model simulations replicated these trends except in the boundary stations, where the modelled NH4 was underpredicted.
- Modelled and observed medians compared well with low variation across the model domain. Predictions for FRP were consistently higher than observations although still reflective of an oligotrophic environment.

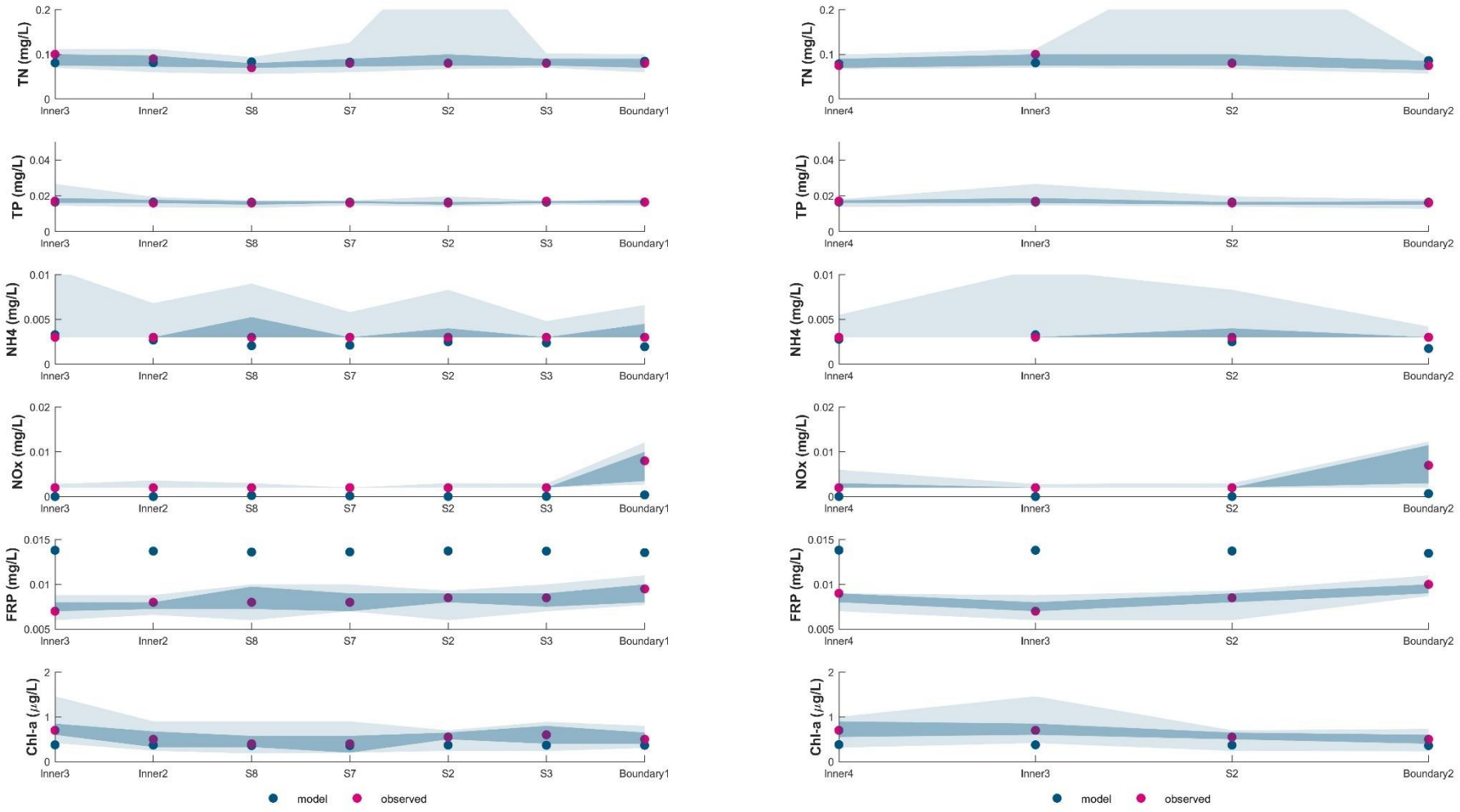


Figure 3.11 Quantile-Quantile comparison of Modelled (Blue) and Recorded (Pink) showing spatial variation of the Surface water quality parameters

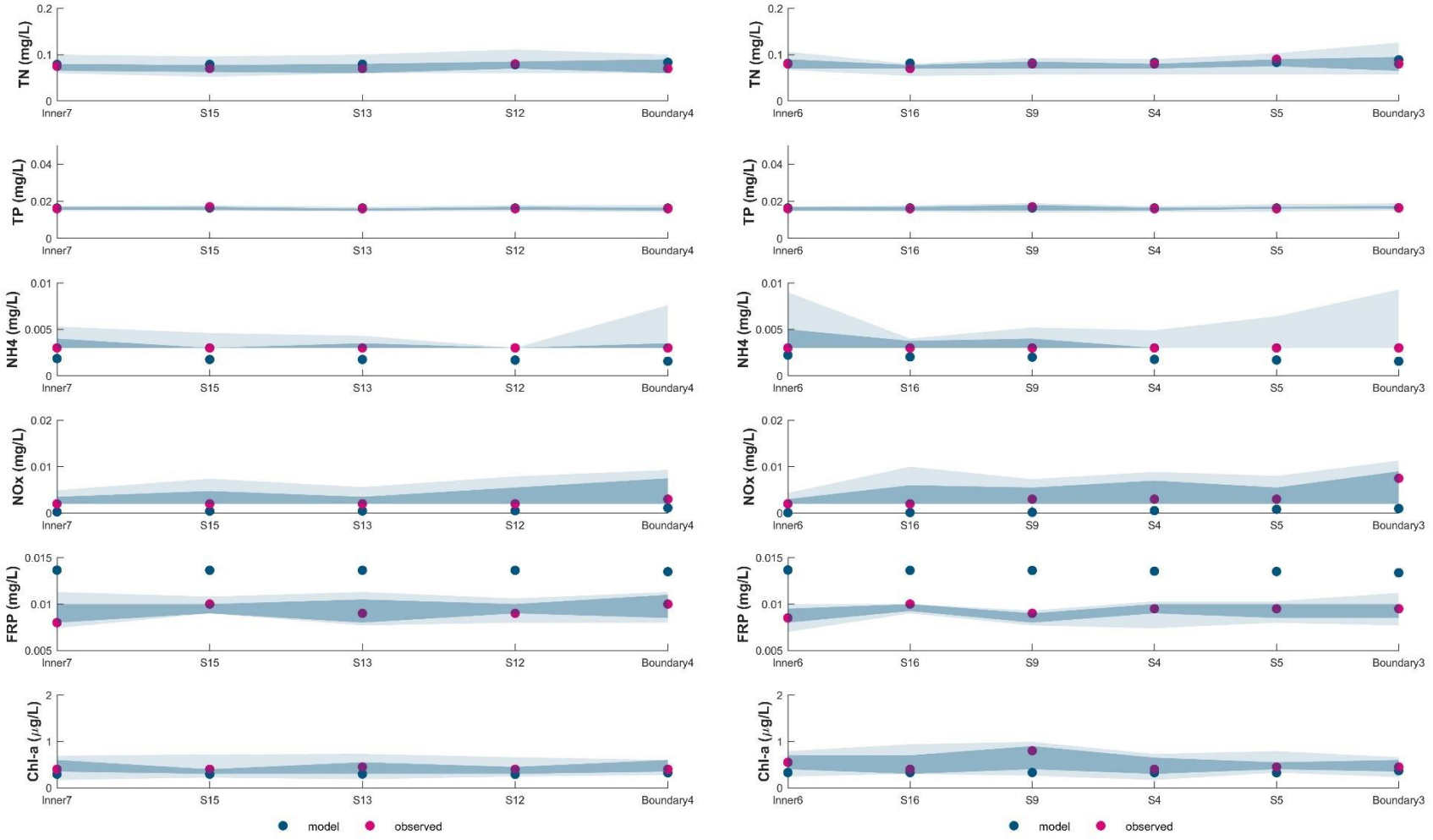


Figure 3.12 Quantile-Quantile comparison of Modelled (Blue) and Recorded (Pink) showing spatial variation of the Surface water quality parameters

# 4 References

BMT (2024a) Ocean Barramundi Project - Marine Environmental Quality Baseline Report. Prepared by BMT for Tassal. Report No. 175801.000_5.

BMT (2024b) Ocean Barramundi Project – Section 38 Referral Supporting Report. Prepared by BMT for Tassal. Report No. 175801.000_1

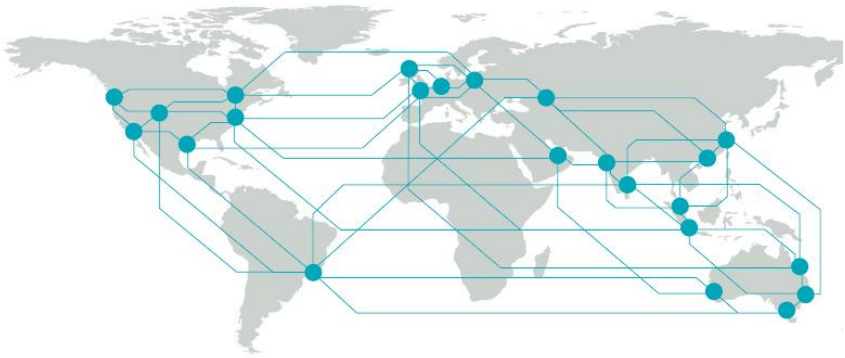

BMT is a leading design, engineering, science and management consultancy with a reputation for engineering excellence. We are driven by a belief that things can always be better, safer, faster and more efficient. BMT is an independent organisation held in trust for its employees.

11 Bon Accord Crescent
Aberdeen
AB11 6DE
Great Britain
+44 (0)1224 414200

Registered in the United Kingdom
Registered no. 02326885
Registered office
Part Level 5, Zig Zag Building,
70 Victoria Street, London,
SW1E 6SQ
+44 20 8943 5544

For your local BMT office visit www.bmt.org

**Contact us**

enquiries@bmtglobal.com

www.bmt.org

**Follow us**

www.bmt.org/linkedin

www.bmt.org/youtube

www.bmt.org/twitter

www.bmt.org/facebook